

Ultrafast dynamics of electrons and phonons: from the two-temperature model to the time-dependent Boltzmann equation

Fabio Caruso^a and Dino Novko^b

^aInstitut für Theoretische Physik und Astrophysik, Christian-Albrechts-Universität zu Kiel, Kiel, Germany; ^bInstitute of Physics, Zagreb, Croatia

ARTICLE HISTORY

Compiled February 16, 2022

ABSTRACT

The advent of pump-probe spectroscopy techniques paved the way to the exploration of the ultrafast dynamics of electrons and phonons in crystalline solids. Following photo-absorption of a pump pulse and the initial electronic thermalization, the dynamics of electronic and vibrational degrees of freedom is dominated by electron-phonon and phonon-phonon scattering processes. The two-temperature model (TTM) and its generalizations – as, e.g., the non-thermal lattice model (NLM) – provide valuable tools to describe these phenomena and the ensuing coupled electron-phonon dynamics over timescales ranging between few hundreds of femtoseconds and tens of picoseconds. While more sophisticated theoretical approaches are nowadays available, the conceptual and computational simplicity of the TTM makes it the method of choice to model thermalization processes in pump-probe spectroscopy, and it keeps being widely applied in both experimental and theoretical studies. In the domain of ab-initio methods, the time-dependent Boltzmann equation (TDBE) ameliorates many of the shortcomings of the TTM and it enables a realistic and parameter-free description of ultrafast phenomena with full momentum resolution. After a pedagogical introduction to the TTM and TDBE, in this manuscript we review their application to the description of ultrafast process in solid-state physics and materials science as well as their theoretical foundation.

1. Introduction

Electron-phonon coupling is one of the fundamental interaction mechanism in solids [1]. It determines the temperature dependence of the electron band structure [2,3] and of the fundamental gap [4], it influences the band effective masses [5] and charge transport [6–8], it underpins the absorption of light in indirect band-gap materials [9,10], plasmon damping [11–13], Kohn anomalies [14–20], the formation of quasiparticles, as e.g. Fröhlich [21–23] and Holstein [24,25] polarons, and it underlies several exotic states of matter, such as superconducting [26–29] and charge-density-wave [30–32] phases. Phonon-assisted scattering processes further govern the ultrafast dynamics of electrons and phonons and determine the time scale for the thermalization of electronic and vibrational degrees of freedom [33]. For example, a photo-excited electron distribution loses its energy by undergoing phonon-assisted scattering processes which entails the emission and absorption of phonons.

Pump-probe experiments provide a versatile tool to directly probe these phenomena

[34,35]. Time- and angle-resolved photoemission spectroscopy, for example, enables to directly probe the dynamics of photoexcited electrons and holes with energy and momentum resolution [36,37]. Additionally, pump-probe scattering techniques as, e.g., ultrafast electron diffuse scattering complement optical and photoemission measurements by providing direct insight into the dynamics of the crystalline lattice and electron-phonon scattering processes with time and momentum resolution, and they are suitable to attain a detailed understanding of the energy flow between hot electrons and the crystalline lattice [38–40].

The two-temperature model (TTM) [41–44] describes the dynamics of electron and phonons as the thermalization involving two coupled thermal reservoirs. This idea provides perhaps the simplest and most intuitive description of the thermalization of electronic and vibrational degrees of freedom in systems out of equilibrium and it has seen wide application to the description of ultrafast processes in solids [38,45–69]. The TTM has been employed to examine the fingerprints of ultrafast dynamics in several experimental techniques including photoemission spectroscopy [70–79], Raman scattering [80,81], ultrafast electron diffuse scattering [38,61,82,83], and pump-probe optical techniques [46,75,84–99]. It has further been extended to account for the emergence of coherent phonons [100,101], ultrafast dynamics in warm-dense matter [58,96,102–105], thermalization via electron-plasmon channel [106], spin dynamics [107], magnon scattering with lattice degrees of freedom [108–113], and thermalization of magnetic-nematic order [114]. An effort has been also made in upgrading the TTM to account for the nascent non-equilibrium electron distribution, while retaining the numerical simplicity of the model [49,88,115,116]. While the application of the TTM to ultrafast electron dynamics in metals and laser ablation has been reviewed in Refs. [117] and [118], respectively, we here focus on its application to coupled electron-phonon dynamics in the context of first-principles simulations. Furthermore, the non-thermal lattice model (NLM), also referred to as N -temperature or multi-temperature model, extends the TTM to account for anisotropies in electron-phonon interaction [38,60,119–121]. In this framework, the lattice is treated as a set of N distinct thermal reservoirs coupled to the electrons. At variance with the TTM, this generalization enables to account for the establishment of *hot phonons* or, more generally, a non-thermal state of the lattice, characterized by the enhanced population of the phonon modes which actively take part in the hot-carrier relaxation [74,76,80,122–125].

A rigorous description of electron-phonon coupling and its influence on the dynamics inevitably requires to account for phase-space constraints in the phonon-assisted scattering processes as well as for the anisotropies of the electron-phonon coupling. A suitable approach to attain this requirement is the time-dependent Boltzmann equation (TDBE). Ultrafast dynamics simulations based on the TDBE formalism have been widely employed to describe non-equilibrium processes involving electrons and phonons in condensed matter. The TDBE has been applied to investigate the thermalization of electrons and phonons following photoirradiation in metals [126–134], semiconductors [135–138], and two-dimensional [139–144] and layered [145] materials, and it has further been extended to investigate the ultrafast magnetization dynamics in photo-excited ferromagnets [146,147]. In comparison to simplified models – as, e.g., the TTM and NLM – a major advantage of the TDBE approach consists in enabling the investigation of the coupled non-equilibrium dynamics of electrons and phonon populations with a full momentum resolution. This aspect is particularly important to capture the anisotropic population of the electronic and vibrational states in reciprocal space which may be established out of equilibrium. For example, the absorption of circularly polarized light in transition metal dichalcogenide monolayers is governed

by valley-selective circular dichroism [148–150]: carriers are photoexcited in either the K or \bar{K} valleys in the Brillouin zone depending on the light helicity, leading to an anisotropic electronic distribution which cannot be captured via a density-of-state approximations [151]. Similarly, highly anisotropic phonon populations in reciprocal space can be established upon the preferential emission of strongly-coupled phonons [143,144], leading to the characteristic spectral signatures in ultrafast diffuse scattering techniques [83,145,152–154].

This manuscript aims at introducing the fundamentals of model approaches and of the time-dependent Boltzmann equation in the context of the non-equilibrium dynamics of coupled electrons and phonons. In particular, in Sec. 2 we introduce the TTM and in Sec. 2.1 its generalization to several temperature reservoirs, i.e., to the NLM. In Sec. 3, we introduce the TDBE and discuss its theoretical foundation (Sec. 3.1) as well as its relation to the TTM. In Sec. 4, after a concise overview of the experimental signatures of non-equilibrium processes in graphene (Sec. 4.1) we proceed to discuss the theoretical description of the ultrafast carrier and lattice dynamics based on the NLM (Sec. 4.2) and the TDBE (Sec. 4.3) approaches. Summary and outlook are discussed in Sec. 5.

2. The two-temperature model

The underlying ideas of the TTM [41–44] are most easily illustrated by considering the thermalization dynamics of two systems S_1 and S_2 . Quantum mechanics is not required at this point; S_1 , S_2 , and their interactions can be assumed to be governed by the laws of thermodynamics. If S_1 and S_2 are initially at thermal equilibrium at the temperatures T_1 and T_2 , respectively, in absence of interactions [Fig. 1 (a)] the temperature of each subsystem will remain unaltered through time [Fig. 1 (b)]. If heat can be exchanged [Fig. 1 (c)], on the other hand, one can expect that for a sufficiently small temperature difference $T_2 - T_1$ the energy transferred from S_1 to S_2 (from S_2 to S_1) during the interval Δt will be linear in $T_2 - T_1$ ($T_1 - T_2$), leading to [41]:

$$\frac{\Delta E_1}{\Delta t} = g_1(T_2 - T_1) \quad , \quad (1)$$

$$\frac{\Delta E_2}{\Delta t} = g_2(T_1 - T_2) \quad . \quad (2)$$

Here, the energy of S_1 is given by $E_1 = c_1 T_1$, where c_1 is the specific heat, and similarly for S_2 . g_1 and g_2 are proportionality constants with units of [energy \times (temperature \times time) $^{-1}$]. Energy conservation throughout the thermalization dynamics requires $\Delta E_1 = -\Delta E_2$, which in turn promptly leads to condition $g_1 = g_2 = g$. In the limit of infinitesimal time interval, the thermalization dynamics of S_1 and S_2 can thus be formulated by the coupled first-order differential equations:

$$\frac{\partial T_1}{\partial t} = \frac{g}{c_1}(T_2 - T_1) \quad , \quad (3)$$

$$\frac{\partial T_2}{\partial t} = \frac{g}{c_2}(T_1 - T_2) \quad . \quad (4)$$

Equations (3) and (4) are the central equations of the two-temperature model. If the temperature dependence of c_1 and c_2 are neglected, Eqs. (3) and (4) admit analytical

solutions in the form of decaying exponentials (see Appendix). A detailed discussion of the analytical solution of the TTM can be found in Ref. [57]. The resulting time dependence of the temperatures T_1 and T_2 is illustrated in Fig. 1 (d). In short, the presence of a coupling constant g tends to restore a regime of thermal equilibrium where $T_2 = T_1$. More generally, owing to the non-trivial temperature dependence of the specific heat, the TTM must be solved numerically via time-stepping algorithms (e.g., the Euler or Runge-Kutta algorithms).

The TTM is often modified to introduce a time-dependent source (driving) term coupled to S_1 or S_2 [50,155]. This scenario is clearly reminiscent of pump-probe experiments [Fig. 1 (e)] whereby either electrons or lattice are driven out of equilibrium through the coupling to ultrashort pulses. If a coupling in the form $S(t) = \alpha e^{-\frac{|t|}{\tau}} \theta(t)$ is added to Eq. (4), i.e., a laser pulse with the amplitude of α that lasts for time period of τ and starts at $t = 0$, the model still admits analytic solution (Appendix), leading to the trend illustrated in Fig. 1 (f). For a more detailed discussion on the time-dependent source term and its different functional forms we refer the reader to the Refs. [49,60,118]. The initial increase of T_2 reflects the raise of temperature of S_2 induced by the interaction with a source, whereas at a later stage, the thermalization follows a similar trend to that of Fig. 1 (d).

The TTM can be straightforwardly employed to model the coupled electron-phonon phonon dynamics in condensed matter via the following steps [44,50]: one of the subsystems (S_1) is identified with lattice, whereas the other (S_2) with the electrons. The temperatures T_1 and T_2 are identified with the effective temperatures of the lattice (T_{ph}) and electrons (T_{el}) and the source term $S(t)$ is employed to model the coupling to an external light source. c_1 and c_2 are replaced by the phonon (C_{ph}) and electron (C_{el}) heat capacities, which can be expressed as [50]:

$$C_{\text{el}}(T) = \int_{-\infty}^{\infty} d\varepsilon D_{\text{el}}(\varepsilon) \varepsilon \frac{\partial f(\mu, \varepsilon, T_{\text{el}})}{\partial T_{\text{el}}} \quad , \quad (5)$$

$$C_{\text{ph}}(T) = \int_0^{\infty} d\omega D_{\text{ph}}(\omega) \omega \frac{\partial n(\omega, T_{\text{ph}})}{\partial T_{\text{ph}}} \quad , \quad (6)$$

where D_{el} and D_{ph} are the electron and phonon density of states. Similarly, the coupling constant g can be expressed as [1,50]:

$$g = \frac{\pi k_B}{\hbar D_{\text{el}}(\varepsilon_F)} \lambda \langle \omega^2 \rangle \int_{-\infty}^{\infty} d\varepsilon D_{\text{el}}^2(\varepsilon) \left(-\frac{\partial f(\mu, \varepsilon, T_{\text{el}})}{\partial \varepsilon} \right) \quad , \quad (7)$$

where the thermalization rate of electron-lattice system is governed by the electron-phonon coupling strength and second moment of the phonon spectrum, which are related to the Eliashberg function $\alpha^2 F(\Omega)$ as $\lambda \langle \omega^2 \rangle = 2 \int d\Omega \Omega \alpha^2 F(\Omega)$. The equations of the TTM, i.e., Eqs. (3) and (4), can thus be expressed as:

$$\frac{\partial T_{\text{ph}}}{\partial t} = \frac{g}{C_{\text{ph}}} (T_{\text{el}} - T_{\text{ph}}) \quad , \quad (8)$$

$$\frac{\partial T_{\text{el}}}{\partial t} = \frac{g}{C_{\text{el}}} (T_{\text{ph}} - T_{\text{el}}) + S(t) \quad . \quad (9)$$

The theoretical foundation of the TTM, and its relation to the TDBE is discussed in Sec. 3.2. While the electron and phonon heat capacities C_{el} and C_{ph} can be im-

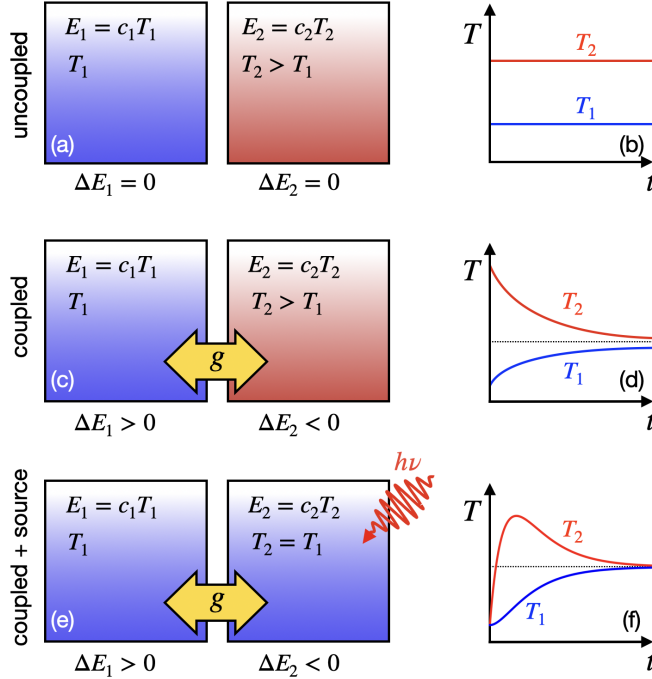


Figure 1. Schematic representation of two thermal reservoirs at temperatures T_1 and $T_2 > T_1$ and energies $E_1 = C_1 T_1$ and $E_2 = C_2 T_2$ – where C_1 and C_2 denote the heat capacities – in absence of interactions (a), in presence of mutual interactions characterized by a coupling constant g (c), and in presence of an external field (e). (b), (d), and (f): Time dependence of the temperature for the systems in (a), (c), and (e), respectively, as obtained from the solution of the TTM.

mediately obtained from calculations based on density-functional theory and density-functional perturbation theory [156], respectively, the parameters g can be estimated from first-principles calculations of the Eliashberg function via well-established simulation packages [157]. This procedure enables the solution of the TTM entirely ab-initio, without resorting to free parameters [50,55,62,68,79]. Alternatively, the g can be deduced by experimental data, e.g., by fitting Eq. (9) to pump-probe photoemission measurements (see, e.g., Sec. 4) [76].

As discussed in Sec. 3.2, the application of the TTM to the non-equilibrium dynamics of electrons and phonons in solids can be justified through its formal derivation from the time-dependent Boltzmann equation [44]. The description of ultrafast processes via Eqs. (3) and (4), however, entails two main approximations: (i) at each time steps throughout the dynamics, electrons are assumed to populate electronic bands according to a Fermi-Dirac function at the effective temperature T_{e1} ; (ii) the lattice is assumed to be at thermal equilibrium throughout the dynamics, i.e., all bosonic occupations are described by the Bose-Einstein statistics at the effective temperature T_{ph} . These approximations limit the domain of applicability of the TTM. Because of the approximation (i), the TTM is unsuitable to describe the early stages of the electron dynamics ($t < 100$ fs), which can be characterized by population inversion, the anisotropic excitation of electron-hole pairs in the Brillouin zone, and electron-electron scatterings. The domain of application of the TTM is thus restricted to metals, semimetals, and doped semiconductors with short electron thermalization times, since, on the other hand, electronic excitations in gapped systems (e.g., semiconductors) are inherently linked to a regime of population inversion that cannot be properly

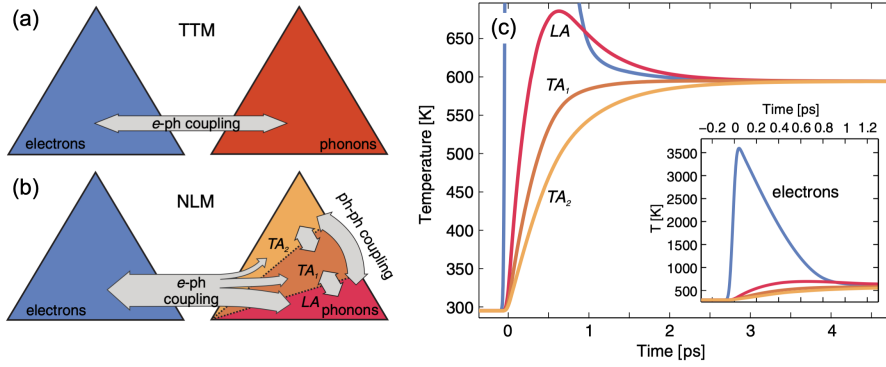


Figure 2. (a) Schematic illustration of the TTM and (b) NLM. At variance with the TTM, the NLM accounts for coupling with different subsets of phonon modes, as well as phonon-phonon interactions. (c) Time-dependence of the electronic (blue) and vibrational temperatures of the longitudinal (LA) and transverse acoustic phonons (TA₁ and TA₂) of aluminum. Reproduced from Ref. [38].

modeled via a Fermi-Dirac function. Additionally, the approximation (ii) makes the TTM unsuitable to describe the non-equilibrium dynamics of the lattice. The TTM is sometimes extended to model the population inversion and other forms of nascent non-equilibrium distributions by defining separately electron and hole thermal baths [158], i.e., electron and hole temperatures [159], or by dividing the electronic bath into a majority of thermal and a small portion of non-thermal carriers [49,88,115,116]. However, in these extensions, the issue of thermalized lattice bath (ii) is still present. In the following, we discuss how this limitation can be overcome by extending the TTM to account for anisotropic coupling to different phonon modes.

2.1. The non-thermal lattice model

Ultrafast diffuse-scattering experiments and first-principles calculations provide strong evidence that non-thermal regimes of the lattice – i.e., vibrational states characterized by bosonic occupations which deviate significantly from the Bose-Einstein statistics – can be established upon photo-excitation in both semiconducting and metallic layered compounds, such as, black phosphorus [145], MoS₂ [144], graphite [83], graphene [143], and TiS₂ [152]. Even for simple metals such as Al, the anisotropic coupling between electrons and acoustic phonons can trigger the emergence of a non-equilibrium vibrational states persisting for several picoseconds [38]. Generally, whenever the electron-phonon interaction is dominated by one or several strongly-coupled modes, these lattice vibrations may provide a preferential decay channel for the relaxation of photo-excited electrons and holes [79]. As mentioned in the introduction, such a scenario can lead to the formation of *hot phonons*, i.e., a non-thermal state of the lattice [74,76,80,124,125]. Because of the assumption that the lattice can be described by a Bose-Einstein distribution at temperature T_{ph} , the TTM is unsuitable to describe these phenomena [38,83,145]

To enable the description of hot phonons and non-thermal states of the lattice, a generalization of the TTM to account for anisotropies in the coupling with different subsets of lattice vibrations – referred to as non-thermal lattice model (NLM) [38,60,120,121] or three-temperature model [79,80], depending on the level of approximation – has recently been proposed. In short, while in the TTM the electrons are coupled to the lattice via a single coupling constant g [Fig. 2 (a)], in the NLM the

lattice is partitioned into phonon groups characterized by distinct coupling constants g_μ [Fig. 2 (b)]. Phonons characterized by higher coupling play a primary role in the electronic relaxation, and therefore exhibit a larger effective temperature on short timescales, whereas on longer timescales thermal equilibrium is restored by phonon-phonon coupling. This behaviour is schematically illustrated in Fig. 2 (c) for aluminum, where only three acoustic phonons are present.

In general, by partitioning the N_{ph} normal modes of the lattice into N_g groups, where $1 < N_g \leq N_{\text{ph}}$ (for $N_g = 1$, the TTM is recovered), the total energy can be expressed as $E_{\text{ph}} = \sum_{\mu=1}^{N_g} E_{\text{ph}}^\mu$. The rate of change of the energy of the μ -th phonon group can be expressed as $\partial_t E_{\text{ph}}^\mu = C_{\text{ph}}^\mu \partial_t T_{\text{ph}}^\mu$, where C_{ph}^μ is the specific heat of the μ -th phonon group, which is obtained by replacing the group density of states in Eq. (6). The NLM can thus be formulated as a set of coupled first-order differential equations which relates the electronic temperature T_{el} to the temperatures T_{ph}^μ of the N_g phonon groups:

$$\frac{\partial T_{\text{ph}}^\mu}{\partial t} = \frac{g_\mu}{C_{\text{ph}}^\mu} (T_{\text{el}} - T_{\text{ph}}^\mu) + \sum_{\mu'} \frac{T_{\text{ph}}^{\mu'} - T_{\text{ph}}^\mu}{\tau_{\mu\mu'}} \quad , \quad (10)$$

$$\frac{\partial T_{\text{el}}}{\partial t} = \sum_{\mu} \frac{g_\mu}{C_{\text{el}}} (T_{\text{ph}}^\mu - T_{\text{el}}) + S(t) \quad . \quad (11)$$

Here, the coupling constant g_μ is defined as in Eq. (7) by restricting the sum to all phonons in the μ -th group, $\tau_{\mu\mu'}$ denotes the time constant for the decay of the μ -th subgroup due to phonon-phonon interaction with phonons in the μ' -th group, and it can be obtained from first-principles via calculations of the phonon-phonon scattering matrix elements [60].

As illustrated in Fig. 2 (c) for Al [38], at variance with TTM, the NLM enables to account for the establishment of a non-thermal regime in the lattice. In particular, following photo-excitation of the electrons, energy is transferred to each phonon group μ proportionally to the coupling constant g_μ , thus, leading to a discrepancy among the vibrational temperatures T_{ph}^μ . On longer timescales, the onset of phonon-phonon scattering (via the second term in Eq. (10)), drives the lattice back to a thermalized regime, where all vibrational temperatures coincides.

With the exception of elemental metals, where the identification of different phonon groups is straightforward due to the reduced vibrational degrees of freedoms (see, e.g., Fig. 2), in compounds with several atoms in the unit cell the definition of phonon groups is to some extent arbitrary, and it represents a shortcoming of the NLM. In some limiting cases (e.g., cuprates, graphene, and MgB₂ [74,79,80]), it is possible to distinguish strongly and weakly coupled modes and, correspondingly, phonons can be grouped according to their coupling strength. The arbitrariness in the definition of phonon groups can be lifted by resorting to a first-principles description of the ultrafast dynamics of electrons and phonons based on the time-dependent Boltzmann equation.

3. The time-dependent Boltzmann equation

The time-dependent Boltzmann equation (TDBE) constitutes an optimal compromise between accuracy and efficiency to investigate the ultrafast dynamics of coupled

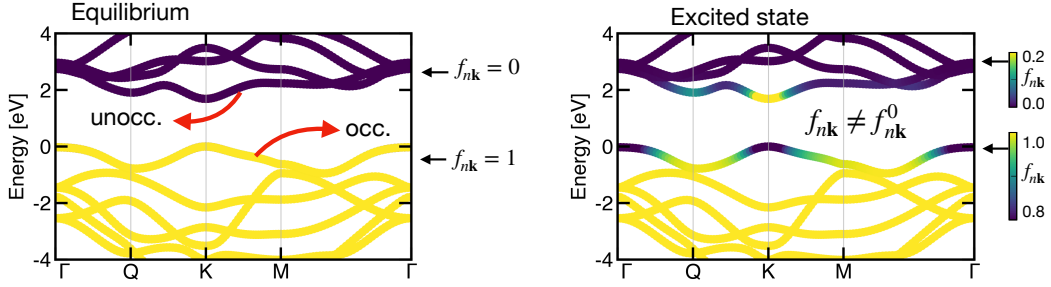


Figure 3. Electron distribution function $f_{n\mathbf{k}}$ superimposed to the band structure of monolayer MoS₂. Energies are relative to the Fermi level. At equilibrium (left), bands are occupied according to the Fermi-Dirac statistics (Eq. (12)). Adapted from Ref. [144].

electron-phonon systems. In the TDBE, the dynamics of electronic and vibrational excitations are described by changes of the electron and phonon distribution functions $f_{n\mathbf{k}}(t)$ and $n_{\mathbf{q}\nu}(t)$, respectively, whereas electron and phonon energies are left unchanged throughout the dynamics. At thermal equilibrium, $f_{n\mathbf{k}}$ and $n_{\mathbf{q}\nu}$ are time independent and they coincide with the Fermi-Dirac and the Bose-Einstein occupations $f_{n\mathbf{k}}^0$ and $n_{\mathbf{q}\nu}^0$:

$$f_{n\mathbf{k}}^0(T) = \left[e^{(\varepsilon_{n\mathbf{k}} - \varepsilon_F)/k_B T} + 1 \right]^{-1}, \quad (12)$$

$$n_{\mathbf{q}\nu}^0(T) = \left[e^{\hbar\omega_{\mathbf{q}\nu}/k_B T} - 1 \right]^{-1}. \quad (13)$$

Here, ε_F is the Fermi energy, $\varepsilon_{n\mathbf{k}}$ is the single-particle energy of a Bloch electron, and $\hbar\omega_{\mathbf{q}\nu}$ the phonon energy. This case is exemplified by the left panel of Fig. 3, where the Fermi-Dirac occupations are superimposed to the band structure of monolayer MoS₂, with yellow (blue) denoting fully occupied (empty) states with $f_{n\mathbf{k}} = 1$ ($f_{n\mathbf{k}} = 0$). In this framework, a regime of non-equilibrium requires either $f_{n\mathbf{k}}$ or $n_{\mathbf{q}\nu}$ (or both) to differ from the equilibrium Fermi-Dirac and the Bose-Einstein occupations, as illustrated in the right panel of Fig. 3. The non-equilibrium distributions change over time, and their dynamics is determined by the TDBE:

$$\partial_t f_{n\mathbf{k}}(t) = \Gamma_{n\mathbf{k}}(t) \quad (14)$$

$$\partial_t n_{\mathbf{q}\nu}(t) = \Gamma_{\mathbf{q}\nu}(t), \quad (15)$$

where $\partial_t = \partial/\partial t$ and $\Gamma_{n\mathbf{k}}$ and $\Gamma_{\mathbf{q}\nu}$ denote the collision integrals for electrons and phonons. The numerical solution of Eqs. (14) and (15) requires the development of suitable approximations for the evaluation of the collision integrals. In short, $\Gamma_{n\mathbf{k}}$ and $\Gamma_{\mathbf{q}\nu}$ account for the several scattering mechanisms which may lead to changes of the distributions functions as, e.g., electron-electron, electron-phonon, phonon-phonon, and impurity scattering as well as the coupling to external fields. The recent development of electronic structure codes for the study of electron-phonon and phonon-phonon coupling has enabled to estimate the contribution of these scattering processes to collision integrals, enabling the investigation of the coupled electron-phonon dynamics entirely from first principles [33,59,134,143,144].

3.1. First-principles expressions for the collision integrals

In the following, we outline the derivation of the collision integral due to the electron-phonon and phonon-phonon interactions from Fermi's golden rule. A similar treatment can be generalized to other contributions to the collision integral as, e.g., electron-electron and impurity scattering or coupling to external fields. The Hamiltonian for an anharmonic crystal in presence of electron-phonon and phonon-phonon interactions can be expressed as:

$$\hat{H} = \hat{H}_e + \hat{H}_p + \hat{H}_{ep} + \hat{H}_{pp} \quad . \quad (16)$$

Here $\hat{H}_e = \sum_{n\mathbf{k}} \varepsilon_{n\mathbf{k}} \hat{c}_{n\mathbf{k}}^\dagger \hat{c}_{n\mathbf{k}}$ is the electronic Hamiltonian, where $\hat{c}_{n\mathbf{k}}^\dagger$ and $\hat{c}_{n\mathbf{k}}$ are fermionic creation and annihilation operators, respectively. $\hat{H}_p = \sum_{\mathbf{q}\nu} \hbar\omega_{\mathbf{q}\nu} [\hat{a}_{\mathbf{q}\nu} \hat{a}_{\mathbf{q}\nu}^\dagger + 1/2]$ is the Hamiltonian of the lattice in the harmonic approximation. $\hat{a}_{\mathbf{q}\nu}^\dagger$ and $\hat{a}_{\mathbf{q}\nu}$ are phonon creation and annihilation operators. The eigenstates of \hat{H}_p can be expressed as $|\chi_s\rangle = \prod_{\mathbf{q}\nu} |n_{\mathbf{q}\nu}^s\rangle$, where $|n_{\mathbf{q}\nu}^s\rangle$ are the eigenstates of the number operator $\hat{N}_{\mathbf{q}\nu} = \hat{a}_{\mathbf{q}\nu}^\dagger \hat{a}_{\mathbf{q}\nu}$ with eigenvalue $n_{\mathbf{q}\nu}^s$. The quantity $n_{\mathbf{q}\nu}^s$ is the occupation number of the bosonic mode characterized by quantum numbers ν and \mathbf{q} . The superscript s -th indicates that the occupations are relative to the s -th eigenstate $|\chi_s\rangle$ of the harmonic Hamiltonian. With this notation, the energy of the harmonic lattice can be expressed as $E_s = \langle \chi_s | \hat{H}_p | \chi_s \rangle = \sum_{\mathbf{q}\nu} \hbar\omega_{\mathbf{q}\nu} [n_{\mathbf{q}\nu}^s + 1/2]$.

The third term in Eq. (16) is the electron-phonon coupling Hamiltonian:

$$\hat{H}_{ep} = N_p^{-\frac{1}{2}} \sum_{\substack{nm\nu \\ \mathbf{k}\mathbf{q}}} g_{mn}^\nu(\mathbf{k}, \mathbf{q}) \hat{c}_{m\mathbf{k}+\mathbf{q}}^\dagger \hat{c}_{n\mathbf{k}} [\hat{a}_{\mathbf{q}\nu} + \hat{a}_{-\mathbf{q}\nu}^\dagger] \quad , \quad (17)$$

where N_p is the number of unit cells in the Born-von Kármán (BvK) supercell [1]. The electron-phonon coupling matrix elements $g_{mn}^\nu(\mathbf{k}, \mathbf{q})$ can be derived from first principles within the framework of density-functional perturbation theory and they are defined as $g_{mn}^\nu(\mathbf{k}, \mathbf{q}) = \langle \psi_{m\mathbf{k}+\mathbf{q}} | \Delta_{\mathbf{q}\nu} v^{\text{KS}} | \psi_{n\mathbf{k}} \rangle$, where $\Delta_{\mathbf{q}\nu} v^{\text{KS}}$ is the linear change of the effective Kohn-Sham potential v^{KS} due to a phonon perturbation, and $|\psi_{n\mathbf{k}}\rangle$ are single-particle orbitals, solutions of the single-particle Kohn-Sham equations [1,156].

Finally, the last term in Eq. (16) is the phonon-phonon coupling Hamiltonian, which arises from anharmonicities of the lattice and it can be expressed as [160]:

$$\hat{H}_{pp} = \frac{1}{3!} \sum_{\mathbf{q}\mathbf{q}'\mathbf{q}''} \sum_{\nu\nu'\nu''} \Psi_{\nu\nu'\nu''}^{\mathbf{q}\mathbf{q}'\mathbf{q}''} [\hat{a}_{\mathbf{q}\nu} + \hat{a}_{-\mathbf{q}\nu}^\dagger] [\hat{a}_{\mathbf{q}'\nu'} + \hat{a}_{-\mathbf{q}'\nu'}^\dagger] [\hat{a}_{\mathbf{q}''\nu''} + \hat{a}_{-\mathbf{q}''\nu''}^\dagger] \quad . \quad (18)$$

$\Psi_{\nu\nu'\nu''}^{\mathbf{q}\mathbf{q}'\mathbf{q}''}$ denotes the phonon-phonon scattering matrix elements, which is related to the probability amplitude of three-phonon scattering processes.

The derivation of the collision integrals for the Hamiltonian in Eq. (16) begins with the observation that electron-phonon and phonon-phonon interactions in solids are typically weak and, thus, the terms \hat{H}_{ep} and \hat{H}_{pp} in the Hamiltonian in Eq. (16) can be treated as perturbations. Correspondingly, the rate $\Gamma_{i \rightarrow f}$ of transitions from an initial state $|i\rangle$ to a final state $|f\rangle$ can be obtained via Fermi's golden rule:

$$\Gamma_{i \rightarrow f} = \frac{2\pi}{\hbar} |\langle f | \hat{V} | i \rangle|^2 \delta(E_f^{\text{tot}} - E_i^{\text{tot}}) \quad , \quad (19)$$

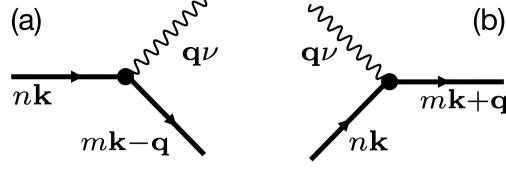


Figure 4. Diagrammatic representation of (a) phonon-emission and (b) phonon-absorption processes. Wavy lines represent non-interacting phonon propagator, whereas straight lines denote non-interacting single-particle propagators.

where E_i^{tot} and E_f^{tot} are the total energies of the initial and final states, respectively, and \hat{V} is an arbitrary perturbation. To proceed further, we focus on the electron-phonon interaction and we consider initial and final states in the form of a Born-Oppenheimer *ansatz* as $|i\rangle = |\Psi_i\rangle|\chi_i\rangle$, where $|\chi_i\rangle$ and $|\Psi_i\rangle$ are eigenstates of the harmonic Hamiltonian \hat{H}_p and of the electronic Hamiltonian \hat{H}_e , respectively. The matrix elements of the electron-phonon coupling Hamiltonian can be expressed as:

$$\langle f|\hat{H}_{\text{ep}}|i\rangle = N_p^{-\frac{1}{2}} \sum_{nm\nu} \sum_{\mathbf{k}\mathbf{q}} g_{mn}^\nu(\mathbf{k}, \mathbf{q}) \langle \Psi_f | \hat{c}_{m\mathbf{k}+\mathbf{q}}^\dagger \hat{c}_{n\mathbf{k}} | \Psi_i \rangle \langle \chi_i | \hat{a}_{\mathbf{q}\nu} + \hat{a}_{-\mathbf{q}\nu}^\dagger | \chi_i \rangle \quad . \quad (20)$$

The matrix elements of fermionic operators in Eq. (20) differs from zero only if $|\Psi_i\rangle$ and $|\Psi_f\rangle$ differ only in the occupation of the $n\mathbf{k}$ and $m\mathbf{k} + \mathbf{q}$ states. In such case, it yields:

$$\langle \Psi_f | \hat{c}_{m\mathbf{k}+\mathbf{q}}^\dagger \hat{c}_{n\mathbf{k}} | \Psi_i \rangle = [f_{n\mathbf{k}}(1 - f_{m\mathbf{k}+\mathbf{q}})]^{\frac{1}{2}} \quad . \quad (21)$$

Similarly, from elementary considerations on the action of bosonic operators on the vibrational eigenstates $|\chi_s\rangle$, one can deduce that the matrix element $\langle \chi_f | \hat{a}_{\mathbf{q}\nu} | \chi_i \rangle = \sqrt{n_{\mathbf{q}\nu}}$ (and similarly, $\langle \chi_f | \hat{a}_{-\mathbf{q}\nu}^\dagger | \chi_i \rangle = \sqrt{n_{-\mathbf{q}\nu} + 1}$) if the state $|\chi_f\rangle$ differs from $|\chi_i\rangle$ only in the occupation of the phonon $\mathbf{q}\nu$ ($-\mathbf{q}\nu$) such that $n_{\mathbf{q}\nu}^f = n_{\mathbf{q}\nu}^i - 1$ (and $n_{\mathbf{q}\nu}^f = n_{\mathbf{q}\nu}^i + 1$), and it vanishes otherwise. The total rate (number of events per unit time) for the absorption of a phonon with quantum numbers $\mathbf{q}\nu$ can be directly derived from Eq. (19) making use of Eqs. (20) and (21) and summing over all initial and final electronic states:

$$\Gamma_{\mathbf{q}\nu}^{\text{abs}} = \frac{4\pi}{\hbar N_p} \sum_{mn\mathbf{k}} |g_{mn}^\nu(\mathbf{k}, \mathbf{q})|^2 f_{n\mathbf{k}}(1 - f_{m\mathbf{k}+\mathbf{q}}) \delta(\varepsilon_{n\mathbf{k}} + \hbar\omega_{\mathbf{q}\nu} - \varepsilon_{m\mathbf{k}+\mathbf{q}}) n_{\mathbf{q}\nu} \quad . \quad (22)$$

The energy difference between the initial and final states has been expressed as $E_i^{\text{tot}} - E_f^{\text{tot}} = \varepsilon_{n\mathbf{k}} + \hbar\omega_{\mathbf{q}\nu} - \varepsilon_{m\mathbf{k}+\mathbf{q}}$. The diagrammatic representation of a phonon absorption process of this kind is reported in Fig. 4 (b). The same procedure can be repeated by considering phonon emission processes [Fig. 4 (a)], yielding:

$$\Gamma_{\mathbf{q}\nu}^{\text{em}} = \frac{4\pi}{\hbar N_p} \sum_{mn\mathbf{k}} |g_{mn}^\nu(\mathbf{k}, \mathbf{q})|^2 f_{n\mathbf{k}}(1 - f_{m\mathbf{k}+\mathbf{q}}) \delta(\varepsilon_{n\mathbf{k}} - \hbar\omega_{\mathbf{q}\nu} - \varepsilon_{m\mathbf{k}+\mathbf{q}}) (n_{\mathbf{q}\nu} + 1) \quad . \quad (23)$$

The total rate of change in the phonon occupation $n_{\mathbf{q}\nu}$ due to the electron-phonon interactions $\Gamma_{\mathbf{q}\nu}^{\text{ep}}$ can thus be defined as the difference between the rates of phonon

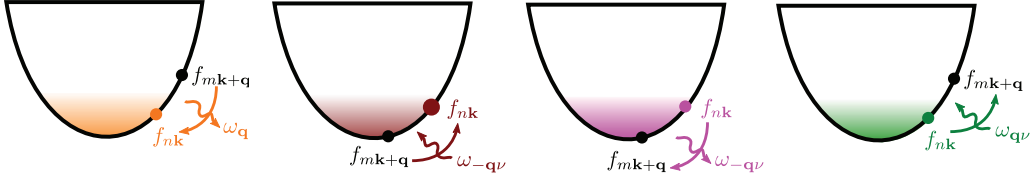


Figure 5. Schematic representation of the four phonon-assisted scattering processes included in the electron collision integral due to the electron-phonon interaction (Eq. (25)). Adapted from Ref. [8].

emission ($\Gamma_{\mathbf{q}\nu}^{\text{em}}$) and absorption ($\Gamma_{\mathbf{q}\nu}^{\text{abs}}$) processes:

$$\Gamma_{\mathbf{q}\nu}^{\text{pe}}(t) = \frac{4\pi}{\hbar N_p} \sum_{mn\mathbf{k}} |g_{mn}^{\nu}(\mathbf{k}, \mathbf{q})|^2 f_{n\mathbf{k}}(1 - f_{m\mathbf{k}+\mathbf{q}}) \times [\delta(\varepsilon_{n\mathbf{k}} - \hbar\omega_{\mathbf{q}\nu} - \varepsilon_{m\mathbf{k}+\mathbf{q}})(n_{\mathbf{q}\nu} + 1) - \delta(\varepsilon_{n\mathbf{k}} + \hbar\omega_{\mathbf{q}\nu} - \varepsilon_{m\mathbf{k}+\mathbf{q}})n_{\mathbf{q}\nu}] \quad (24)$$

Equation (24) is the phonon collision integral due to the electron-phonon interaction. Its time dependence arises from the changes of the electron and phonon distribution functions ($f_{n\mathbf{k}}$ and $n_{\mathbf{q}\nu}$) over time. In conditions of thermal equilibrium between electrons and the lattice, as for instance in an ideal situation in which electron and phonon occupations are described by Fermi-Dirac and Bose-Einstein statistics at a given temperature, the rates $\Gamma_{\mathbf{q}\nu}^{\text{abs}}$ and $\Gamma_{\mathbf{q}\nu}^{\text{em}}$ are equal and opposite in sign, indicating that the total change in the phonon number $n_{\mathbf{q}\nu}$ vanishes, since the emission and absorption of phonons are perfectly compensated.

Following similar steps, the electronic collision integral due to the electron-phonon interaction can be derived as:

$$\Gamma_{n\mathbf{k}}^{\text{ep}}(t) = \frac{2\pi}{\hbar N_p} \sum_{m\nu\mathbf{q}} |g_{mn}^{\nu}(\mathbf{k}, \mathbf{q})|^2 \times \left\{ (1 - f_{n\mathbf{k}})f_{m\mathbf{k}+\mathbf{q}}\delta(\varepsilon_{n\mathbf{k}} - \varepsilon_{m\mathbf{k}+\mathbf{q}} + \hbar\omega_{\mathbf{q}\nu})(1 + n_{\mathbf{q}\nu}) + (1 - f_{n\mathbf{k}})f_{m\mathbf{k}+\mathbf{q}}\delta(\varepsilon_{n\mathbf{k}} - \varepsilon_{m\mathbf{k}+\mathbf{q}} - \hbar\omega_{\mathbf{q}\nu})n_{\mathbf{q}\nu} - f_{n\mathbf{k}}(1 - f_{m\mathbf{k}+\mathbf{q}})\delta(\varepsilon_{n\mathbf{k}} - \varepsilon_{m\mathbf{k}+\mathbf{q}} - \hbar\omega_{\mathbf{q}\nu})(1 + n_{\mathbf{q}\nu}) - f_{n\mathbf{k}}(1 - f_{m\mathbf{k}+\mathbf{q}})\delta(\varepsilon_{n\mathbf{k}} - \varepsilon_{m\mathbf{k}+\mathbf{q}} + \hbar\omega_{\mathbf{q}\nu})n_{\mathbf{q}\nu} \right\} \quad (25)$$

Each term in this expression is directly related to phonon-assisted electronic transitions involving states in the vicinity of the Fermi surface, as depicted in Fig. 5. In particular, the first and second terms in Eq. (25) arise from processes in which an electron scatter from $m\mathbf{k} + \mathbf{q}$ into $n\mathbf{k}$ via the emission and absorption of a phonon, respectively. The third and fourth terms arise from the scattering from $n\mathbf{k}$ into $m\mathbf{k} + \mathbf{q}$ due to phonon-emission and absorption processes. In analogy to Eq. (24), at thermal equilibrium, scattering processes in and out of $n\mathbf{k}$ balance each other, leading to $\Gamma_{n\mathbf{k}}^{\text{ep}} = 0$. Note that the rate $\Gamma_{n\mathbf{k}}^{\text{ep}}$ of electron population relaxation defined with Eq. (25) and the corresponding lifetime $\tau_{n\mathbf{k}}^{\text{ep}} = \hbar/\Gamma_{n\mathbf{k}}^{\text{ep}}$ should not be confused with the quasiparticle decay rate and lifetime as obtained from the imaginary part of the electron self-energy [161]. It is the former and not the latter that is usually extracted from pump-probe measurements.

The derivation of the scattering rate due to the phonon-phonon scattering involves the tedious (but otherwise straightforward) evaluation of several matrix elements of

bosonic operators. The result can be recast in the form:

$$\Gamma_{\mathbf{q}\nu}^{\text{pp}}(t) = \frac{2\pi}{\hbar} \sum_{\nu'\nu''} \int \frac{d\mathbf{q}'}{\Omega_{\text{BZ}}} \left| \Psi_{\mathbf{q}\mathbf{q}'\mathbf{q}''}^{\nu'\nu''} \right|^2 \quad (26)$$

$$\times \left[[(n_{\mathbf{q}\nu} + 1)(n_{\mathbf{q}'\nu'} + 1)n_{\mathbf{q}''\nu''} - n_{\mathbf{q}\nu}n_{\mathbf{q}'\nu'}(n_{\mathbf{q}''\nu''} + 1)] \delta(\omega_{\mathbf{q}\nu} + \omega_{\mathbf{q}'\nu'} - \omega_{\mathbf{q}''\nu''}) \delta_{\mathbf{q}\mathbf{q}'-\mathbf{q}''}^{\mathbf{G}} + \right.$$

$$\left. \frac{1}{2} [(n_{\mathbf{q}\nu} + 1)n_{\mathbf{q}'\nu'}n_{\mathbf{q}''\nu''} - n_{\mathbf{q}\nu}(n_{\mathbf{q}'\nu'} + 1)(n_{\mathbf{q}''\nu''} + 1)] \delta(\omega_{\mathbf{q}\nu} - \omega_{\mathbf{q}'\nu'} - \omega_{\mathbf{q}''\nu''}) \delta_{\mathbf{q}-\mathbf{q}'-\mathbf{q}''}^{\mathbf{G}} \right]$$

where the modified Kronecker's $\delta_{\mathbf{q}}^{\mathbf{G}}$ equals unity if $\mathbf{q} = 0$ or $\mathbf{q} = \mathbf{G}$, where \mathbf{G} is a reciprocal-lattice vector, and it is zero otherwise. Equations (26) vanishes identically if the lattice is at thermal equilibrium.

Combining Eqs. (25)-(26), the time-dependent Boltzmann equation can be rewritten as:

$$\partial_t f_{n\mathbf{k}}(t) = \Gamma_{n\mathbf{k}}^{\text{ep}}[f_{n\mathbf{k}}(t), n_{\mathbf{q}\nu}(t)] \quad , \quad (27)$$

$$\partial_t n_{\mathbf{q}\nu}(t) = \Gamma_{\mathbf{q}\nu}^{\text{pe}}[f_{n\mathbf{k}}(t), n_{\mathbf{q}\nu}(t)] + \Gamma_{\mathbf{q}\nu}^{\text{pp}}[n_{\mathbf{q}\nu}(t)] \quad . \quad (28)$$

A numerical procedure to solve Eqs. (27) and (28) consists in: (i) defining an initial electronic (or vibrational) excited state characterized by electronic (vibrational) occupations which differs from the equilibrium ones (as e.g. in Fig. 3); (ii) solve the differential equation using iterative methods (as, e.g., the Euler or Runge-Kutta methods); (iii) update the collision integrals via Eqs. (25)-(26) at each time step.

Besides the aforesaid microscopic scattering process, electron-electron interaction plays a major role in thermalization of electron-lattice system, especially in the 10-fs timescale. The corresponding collision integral $\Gamma_{n\mathbf{k}}^{\text{ee}}[f_{n\mathbf{k}}(t)]$ enters Eq. (27) and it is usually defined in terms of electron scatterings $\{\mathbf{k}, \mathbf{k}'\} \rightarrow \{\mathbf{k} + \mathbf{q}, \mathbf{k}' - \mathbf{q}\}$ (and vice versa) mediated by the statically screened Coulomb interaction. For a detailed description of electron-electron scattering processes we refer the reader to Refs. [121, 132, 134, 162]. Note that the electron-plasmon scatterings, as a part of the dynamical electron-electron interaction, is as well considered to be essential in the early stage of electron thermalization process [126, 163, 164], however, these dynamical effects are rarely taken into account when studying hot carrier thermalization.

3.2. Relation between the TTM and the time-dependent Boltzmann equation

As demonstrated by Allen [44], the thermalization dynamics of electrons and phonons in presence of the electron-phonon interaction can be recast in the form of a TTM, as formulated via Eqs. (3) and (4), starting entirely from first principles. In short, by expressing the coupling parameter g in terms of the Eliashberg function $\alpha^2 F$, all free parameters of the models are fixed. A detailed derivation of this scheme can be found, for instance, in Refs. [60, 121].

In the following, we report an alternative derivation of the TTM with scope of emphasizing the link with the phonon lifetime, as obtained from phonon self-energy due to the electron-phonon interaction. We begin by considering the total energy of a

set of non-interacting electrons (E_{el}) and phonons (E_{ph}):

$$E_{\text{el}}(t) = N_p^{-1} \sum_n \sum_{\mathbf{k}} \varepsilon_{n\mathbf{k}} f_{n\mathbf{k}}(t) \quad , \quad (29)$$

$$E_{\text{ph}}(t) = N_p^{-1} \sum_{\nu} \sum_{\mathbf{q}} \hbar\omega_{\mathbf{q}\nu} \left[n_{\mathbf{q}\nu}(t) + \frac{1}{2} \right] \quad . \quad (30)$$

The rate of change of the energies can be expressed as:

$$C_{\text{el}} \partial_t T_{\text{el}} = N_p^{-1} \sum_n \sum_{\mathbf{k}} \varepsilon_{n\mathbf{k}} \partial_t f_{n\mathbf{k}} \quad . \quad (31)$$

$$C_{\text{ph}} \partial_t T_{\text{ph}} = N_p^{-1} \sum_{\nu} \sum_{\mathbf{q}} \hbar\omega_{\mathbf{q}\nu} \partial_t n_{\mathbf{q}\nu} \quad , \quad (32)$$

where $\partial_t = \partial/\partial t$, the left-hand side has been rewritten making use of the chain rule $\partial_t E = \frac{\partial E}{\partial T} \frac{\partial T}{\partial t}$, and the heat capacity $C_{\text{el(ph)}} = \partial E_{\text{el(ph)}}/\partial T_{\text{el(ph)}}$ has been introduced. Equations (31) and (32) rely on the assumption that electron energies $\varepsilon_{n\mathbf{k}}$ and phonon frequencies $\omega_{\mathbf{q}\nu}$ do not depend on time. The time derivative of the fermionic and bosonic distribution functions entering Eqs. (31) and (32) can be obtained via the time-dependent Boltzmann equation.

A central assumption of the non-thermal lattice model is that, at each time t , the electronic occupation $f_{n\mathbf{k}}$ can be approximated by a Fermi-Dirac function at temperature T_{el} :

$$f_{n\mathbf{k}} \simeq \{ \exp[(\varepsilon_{n\mathbf{k}} - \mu)/k_{\text{B}}T_{\text{el}}] + 1 \}^{-1} \quad . \quad (33)$$

Similarly, it is assumed that the lattice remains at thermal equilibrium throughout the dynamics, that is, all vibrational modes are at the same temperature T_{ph} (a condition that may be violated in the non-equilibrium dynamics of the lattice following photoexcitation [144]). Under these assumptions, the arguments of the collision integrals can be simplified. For instance, the argument of Eq. (24) can be rewritten as [60]:

$$\begin{aligned} & [(1 - f_{n\mathbf{k}}) f_{m\mathbf{k}+\mathbf{q}} (n_{\mathbf{q}\nu} + 1) - f_{n\mathbf{k}} (1 - f_{m\mathbf{k}+\mathbf{q}}) n_{\mathbf{q}\nu}] \\ & = (f_{m\mathbf{k}+\mathbf{q}} - f_{n\mathbf{k}}) [n_{\text{BE}}(\omega_{\mathbf{q}\nu}, T_{\mathbf{q}\nu}) - n_{\text{BE}}(\omega_{\mathbf{q}\nu}, T_{\text{el}})] \quad , \end{aligned} \quad (34)$$

where we introduced the Bose-Einstein function:

$$n_{\text{BE}}(\omega, T) = [\exp(\hbar\omega/k_{\text{B}}T) - 1]^{-1} \quad . \quad (35)$$

Additionally, we set $\varepsilon_{m\mathbf{k}+\mathbf{q}} - \varepsilon_{n\mathbf{k}} = \hbar\omega_{\mathbf{q}\nu}$ because of the Dirac- δ in Eq. (24), and we used $n_{\mathbf{q}\nu} = n_{\text{BE}}(\omega_{\mathbf{q}\nu}, T_{\text{ph}})$. A Taylor expansion of n_{BE} to first order yields:

$$n_{\text{BE}}(\omega_{\mathbf{q}\nu}, T_{\text{ph}}) - n_{\text{BE}}(\omega_{\mathbf{q}\nu}, T_{\text{el}}) \simeq (T_{\text{ph}} - T_{\text{el}}) \left. \frac{\partial n_{\text{BE}}(\omega_{\mathbf{q}\nu}, T)}{\partial T} \right|_{T=T_{\text{ph}}} = (T_{\text{ph}} - T_{\text{el}}) \frac{c_{\mathbf{q}\nu}}{\hbar\omega_{\mathbf{q}\nu}} \quad .$$

In the last equality, we introduced the specific heat of a single harmonic oscillator $c_{\mathbf{q}\nu} = \hbar\omega_{\mathbf{q}\nu} \partial n_{\mathbf{q}\nu} / \partial T$.

Making use of Eqs. (34), the integrand within the phonon-electron collision integral in Eq. (24) can be rewritten as:

$$\Gamma_{\mathbf{q}\nu}^{\text{pe}} = \frac{c_{\mathbf{q}\nu}}{\hbar\omega_{\mathbf{q}\nu}} \frac{(T_{\text{el}} - T_{\text{ph}})}{\tau_{\mathbf{q}\nu}} . \quad (36)$$

Where we introduced the phonon lifetime due to the electron-phonon interaction [1]:

$$\tau_{\mathbf{q}\nu}^{-1} = \frac{4\pi}{\hbar N_p} \sum_{m\mathbf{k}} |g_{m\nu}(\mathbf{k}, \mathbf{q})|^2 (f_{n\mathbf{k}} - f_{m\mathbf{k}+\mathbf{q}}) \delta(\varepsilon_{m\mathbf{k}+\mathbf{q}} - \varepsilon_{n\mathbf{k}} - \hbar\omega_{\mathbf{q}\nu}) . \quad (37)$$

Via the identity $\tau_{\mathbf{q}\nu}^{-1} = -2\text{Im}\Pi_{\mathbf{q}\nu}$, Eq. (36) further establishes a simple relation between the phonon self-energy due to the electron-phonon interaction $\Pi_{\mathbf{q}\nu}$ and the corresponding collision integral. The limit of validity of this identity are defined by the assumptions made thus far. Combining (37) with Eq. (32):

$$C_{\text{ph}}\partial_t T_{\text{ph}} = N_p^{-1} \sum_{\nu} \sum_{\mathbf{q}} c_{\mathbf{q}\nu} \frac{(T_{\text{el}} - T_{\text{ph}})}{\tau_{\mathbf{q}\nu}} . \quad (38)$$

A similar identity can be derived by applying the same procedure for the electronic term. After introducing the effective electron-phonon coupling constant g :

$$g = N_p^{-1} \sum_{\nu} \sum_{\mathbf{q}} \frac{c_{\mathbf{q}\nu}}{\tau_{\mathbf{q}\nu}} , \quad (39)$$

the equations of the TTM, Eq. (3) and (4) are recovered.

4. Ultrafast carrier dynamics in graphene

Graphene constitutes a paradigmatic example to introduce the hot-carrier dynamics revealed by pump-probe experiments in 2D materials. Ultrafast phenomena in graphene have been extensively investigated experimentally to explore its suitability for optoelectronic applications and light harvesting. Additionally, a recent discovery of the light-induced Hall effect has revealed a novel route to trigger a non trivial topological behaviour using light pulses [165–167]. The first ultrafast experimental studies resorted to optical techniques [122,158,159,168–176]. Subsequently, time- and angle-resolved photoemission spectroscopy (tr-ARPES) enabled to directly monitor the non-equilibrium dynamics of photo-excited carriers with momentum resolution [76–78,123,177–184]. Despite over a decade of extensive research, ultrafast hot carrier dynamics in graphene is still actively explored [68,79,95,185–190].

4.1. Experimental signature of hot-carrier dynamics in graphene

The ultrafast dynamics of Dirac carriers in pump-probe experiments is usually approximated as a four-step process consisting of (i) photo-excitation, (ii) formation of a quasi-equilibrium state, (iii) full electron thermalization, and (iv) energy transfer to the lattice (acoustic phonons). In the step (i), the interaction with a pump pulse drives the system into an electronic excited state, with carriers photo-excited above

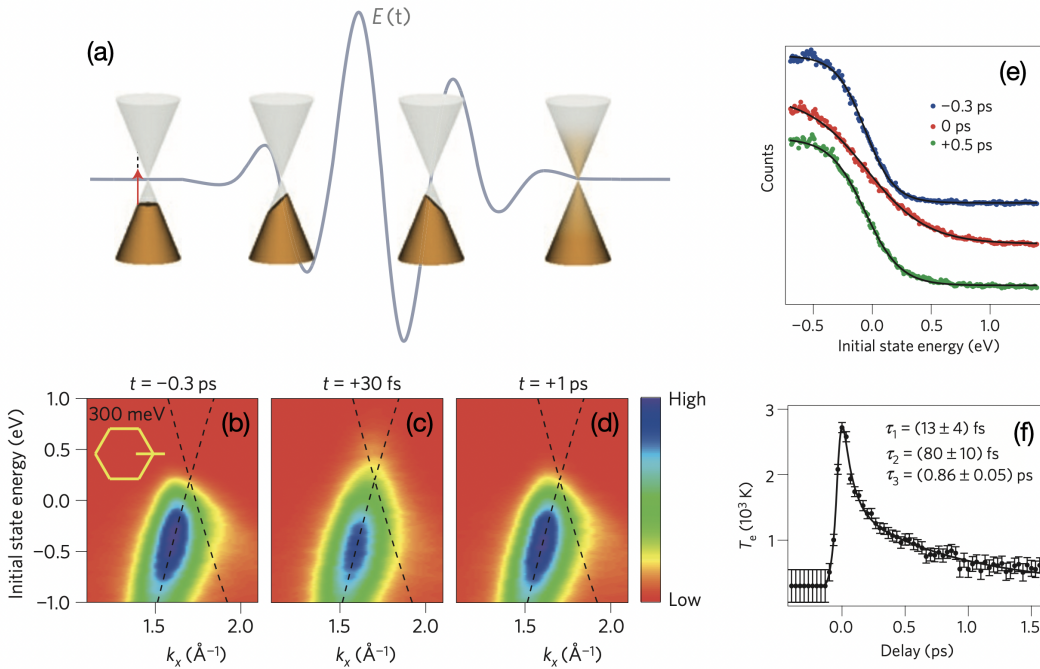


Figure 6. (a) Schematic representation of the thermalization dynamics of electrons and holes following photo-excitation in the vicinity of the Dirac cone of graphene. Time and angle-resolved photoemission spectral function of doped graphene before photo-excitation (b), and at time delays $t = 30$ fs (c), and $t = 1$ ps (d). Momentum integrated spectral function (e) and, superimposed as a continuous line, the Fermi-Dirac function at the effective electronic temperature T_e . (f) Time-dependent effective electronic temperature derived by the fitting procedure illustrated in (e). Adapted from Ref. [77].

the Fermi level. With this a non-equilibrium electron distribution is created. The step (ii) involves electron-electron scatterings, impact ionization, and Auger processes (timescale of ~ 10 fs) [162,191], which promote photo-excited electrons and holes towards the Fermi level. Some experiments indicate that under suitable conditions a regime of population inversion can be established, i.e., two electron distributions with separate chemical potentials (and temperatures) [77,192]. Interestingly, some theoretical works suggested that strong scatterings between non-equilibrium electrons and phonon are active already at this stage [132,193]. Even more, this early electron-phonon scattering process might be responsible for majority of energy flow, leaving a small portion of excess energy for the later scatterings between equilibrium electrons and phonons [132]. In step (iii), Auger recombination [172,194], scatterings with optical phonons [76,122], as well as plasmon emission [163,164] bring the electrons to a thermalized regime (~ 100 fs), where the electronic distribution function is described by a high-temperature Fermi-Dirac function. Finally, in step (iv), the photo-excited electrons and holes dissipate their energy via phonon-assisted scattering processes, mostly via the acoustic modes ($\sim 1 - 10$ ps). Supercollisions [76] and the formation of hot phonons [195] have been proposed as underlying physical processes to explain the energy transfer to the lattice [122,196]. Further experimental investigations on the parent compound graphite corroborated the hot-phonon picture [37,197]. Overall, these studies revealed a complex non-equilibrium dynamics characterized by the coexistence of several scattering mechanisms which are challenging to decipher based on purely experimental investigations.

Exemplary tr-ARPES experiments on hole-doped graphene are illustrated in Fig. 6

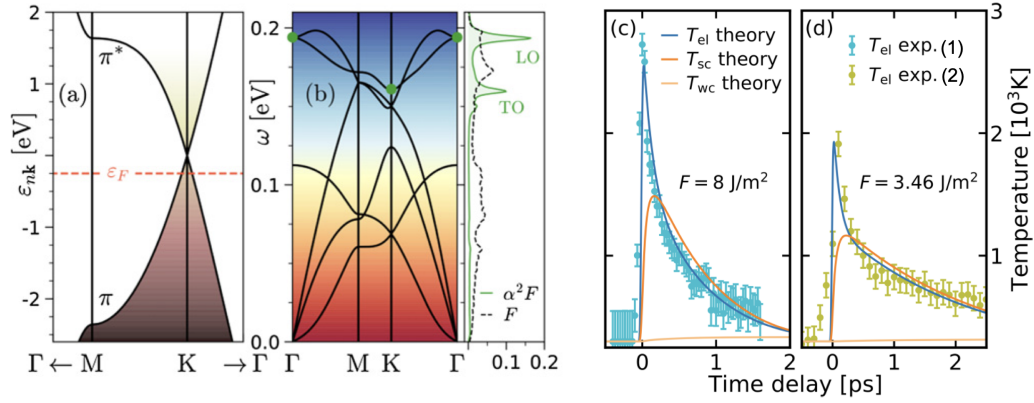


Figure 7. (a) DFT Band structure of graphene in the vicinity of the Dirac cone along the M-K high-symmetry path in the Brillouin zone. (b) Left: Phonon dispersion of graphene obtained from DFPT. Right: Phonon density of states (F) and Eliashberg function ($\alpha^2 F$) of graphene. The peaks at 0.16 and 0.19 eV reflect the strong coupling to transverse optical (TO) and longitudinal optical (LO) phonons in the vicinity of the K and Γ points, respectively [green dots in panel (b)]. (c-d) Pump-probe photoemission measurements of the effective electronic temperature T_{el} of graphene (dots) for photo-excitation fluences $F = 8 \text{ J/m}^2$ (c) and $F = 3.46 \text{ J/m}^2$ from Refs. [76,77]. Simulations based on the NLM (more precisely, three-temperature model) with first-principles parameters are reported as continuous lines. Panels (a-b) and (c-d) are adapted from Ref. [68] and Ref. [79], respectively.

[77]. As a result of substrate-induced hole-doping, the Fermi energy is located 0.2 eV below the Dirac point [Fig. 6 (a)]. Figures 6 (b-d) illustrate several time snapshots of the tr-ARPES spectral function in the vicinity of the Dirac point. Before excitation [Fig. 6 (b)], the spectral intensity reflects occupied electronic states at equilibrium, with broadening arising from finite temperature and experimental resolution. Owing to the optical selection rules governing the coupling with linearly-polarized light, the spectral intensity is dominated by contributions arising from the left sub-band [198]. The change in spectral intensity for $t = 30 \text{ fs}$ [Fig. 6 (c)] reflects the excitation of carriers above the Fermi level, whereas measurements at longer time delays [Fig. 6 (d)] indicates the recovery of an equilibrium regime.

High-quality tr-ARPES measurements can be analysed to extract the effective electronic temperatures T_{el} and its time dependence [71,72,76,77,123,199–201], thus, establishing a direct link with the TTM and NLM discussed in Secs. 2 and 2.1. For a given time delay, T_{el} can be determined by fitting the normalized momentum-integrated photoemission intensity with a Fermi-Dirac function. This procedure is illustrated in Fig. 6 (e) where the fit Fermi-Dirac function (continuous line) is superimposed to the measured energy distribution curves (dots). The time dependence of T_{el} , shown in Fig. 6 (f), is obtained by repeating this procedure for several measured time delays and it closely resembles the trend reported for the light-driven TTM illustrated in Fig. 1 (c): the photo-excitations of the electrons by the pump pulse manifests itself through the initial increase of electronic temperature, whereas the subsequent cooling reflects the thermalization dynamics due electron-phonon scattering processes.

4.2. Theoretical modelling of carrier thermalization in graphene

First-principles calculations of the electron-phonon interaction can be combined with the time-propagation algorithms discussed in Secs. 2-3 to investigate the origin of the hot-carrier dynamics and its fingerprints in spectroscopy. The band structure and

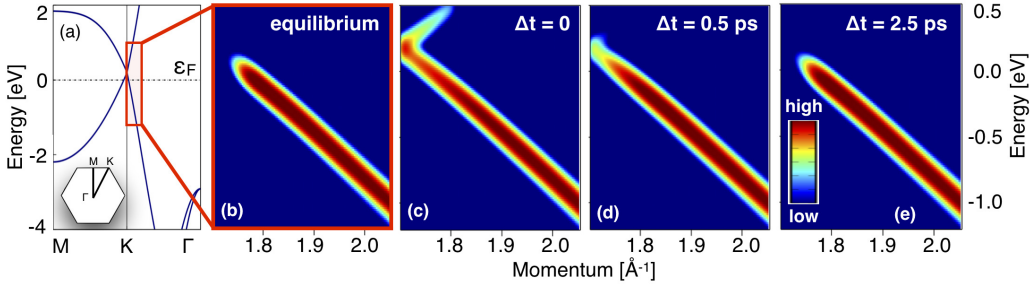


Figure 8. (a) DFT Band structure of graphene in the vicinity of the Dirac cone. The dashed line denotes the Fermi energy $\varepsilon_F = -0.2$ eV, corresponding to a carrier concentration $8 \times 10^{12} \text{ cm}^{-2}$. The inset illustrates the hexagonal Brillouin zone. First-principles calculations of the time- and angle-resolved spectral function obtained by considering electronic and vibrational occupations derived from the solution of the TTM before excitation (b), and at time delays $\Delta t = 0$ (c), $\Delta t = 0.5$ ps (d), and $\Delta t = 2.5$ ps (e). Reproduced from Ref. [79].

phonon dispersion of hole-doped graphene is illustrated in Fig. 7 (a) and (b), respectively [68], whereas the phonon density of state (F) and the Eliashberg function ($\alpha^2 F$) are shown in the right panel of Fig. 7 (b). The Eliashberg function reflects the weighted phonon density of states, to which individual phonons contribute according to their electron-phonon coupling strength [202]. The sharp peaks in $\alpha^2 F$ at 160 and 190 meV indicate that the electron-phonon coupling arises primarily from longitudinal optical (LO or E_{2g}) phonons at Γ and transverse optical (TO or A'_1) modes at K [green dots in Fig. 7 (b)], whereas remaining phonons couple relatively weakly to the electrons. This finding suggests that a few phonons are likely to provide a preferential decay channel for the relaxation of excited carriers, leading to the emergence of hot phonons – namely, phonons characterized by a higher vibrational temperature. The pronounced anisotropy of the electron-phonon interaction in graphene can be explicitly accounted for by formulating a NLM (i.e., a three-temperature model) which discriminates between strongly- (sc) and weakly-coupled (wc) phonons [79], and by determining the model parameters from first-principles calculations [156,157,203]. The effective electronic temperature T_{el} and the vibrational temperatures (T_{wc} and T_{sc}) obtained from the solution of the NLM [Eqs. (10) and (11)] are illustrated in Figs. 7 (c) and (d) for different excitation conditions [79]. The electronic temperature follows the characteristic trend expected for photoexcited electrons and it is in good agreement with the experimental values extracted from tr-ARPES. The preferential excitation of strongly-coupled modes upon carrier relaxation leads to a pronounced rise of T_{sc} , whereas the vibrational temperatures of weakly-coupled modes T_{wc} is smaller.

By post-processing the effective temperatures T_{el} , T_{wc} , and T_{sc} , one can define a simple procedure to estimate the transient changes of many-body interactions and their signatures in photoemission. The self-energy due to electron-phonon interaction can be modified to account for changes of the electronic and vibrational distribution functions as:

$$\begin{aligned} \Sigma_{n\mathbf{k}}(\omega, \Delta t) &= \frac{1}{N_p} \sum_{m\nu\mathbf{q}} |g_{m\nu}(\mathbf{k}, \mathbf{q})|^2 \\ &\times \left[\frac{n_{\mathbf{q}\nu}(\Delta t) + f_{m\mathbf{k}+\mathbf{q}}(\Delta t)}{\hbar\omega - \tilde{\varepsilon}_{m\mathbf{k}+\mathbf{q}} + \hbar\omega_{\mathbf{q}\nu}} + \frac{n_{\mathbf{q}\nu}(\Delta t) + 1 - f_{m\mathbf{k}+\mathbf{q}}(\Delta t)}{\hbar\omega - \tilde{\varepsilon}_{m\mathbf{k}+\mathbf{q}} - \hbar\omega_{\mathbf{q}\nu}} \right]. \end{aligned} \quad (40)$$

The time dependence arise from the dependence of the electron and phonon distri-

bution functions on the effective temperatures, given by $f_{n\mathbf{k}} = [e^{\varepsilon_{n\mathbf{k}}/k_B T_{el}} + 1]^{-1}$ and $n_{\nu\mathbf{q}} = [e^{\omega_{\nu\mathbf{q}}/k_B T_{\nu}} - 1]^{-1}$, respectively, where $T_{\nu} = T_{sc}$ ($T_{\nu} = T_{wc}$) for the strongly (weakly) coupled modes. The tr-ARPES spectral function can be directly derived from Eq. (40) via $A_{\mathbf{k}}(\omega, \Delta t) = \pi^{-1} \sum_n \text{Im} [\hbar\omega - \varepsilon_{n\mathbf{k}} - \Sigma_{n\mathbf{k}}(\omega, \Delta t)]^{-1}$. The spectral function of graphene obtained from this procedure is illustrated in Fig. 8, and it reproduces the main spectral signatures of photoexcitations revealed by experiments as well as the characteristic time scales of photoexcitations.

Other time-dependent physical features of ultrafast hot carrier cooling visible in pump-probe spectroscopy can be theoretically captured in a similar fashion, i.e., by benefiting from the time dependence of electron and phonon temperatures. For instance, time dynamics of electron excitations (e.g., plasmons and screened interband transitions) immediately after the laser excitation can be simulated via optical conductivity $\sigma(\omega; T_{el}, T_{ph})$ or dielectric function $\epsilon(\mathbf{q}, \omega; T_{el}, T_{ph})$ [88,124]. The spectral function of electron excitations (or the so-called electron energy loss function) is defined as [68,204]

$$-\text{Im} \left[\frac{1}{\epsilon(\mathbf{q}, \omega; T_{el}, T_{ph})} \right] = -\text{Im} \left[\frac{\omega^2}{\omega^2 - \Omega^2(\mathbf{q}, \omega; T_{el}, T_{ph}) + i\Gamma(\mathbf{q}, \omega; T_{el}, T_{ph})} \right], \quad (41)$$

where $\Omega^2(\mathbf{q}, \omega; T_{el}, T_{ph}) = v(\mathbf{q})q^2 \text{Re} \pi_{\alpha\alpha}(\mathbf{q}, \omega; T_{el}, T_{ph})$ and $\Gamma(\mathbf{q}, \omega; T_{el}, T_{ph}) = -v(\mathbf{q})q^2 \text{Im} \pi_{\alpha\alpha}(\mathbf{q}, \omega; T_{el}, T_{ph})$, define the energy and corresponding damping (e.g., Landau damping and electron-phonon channel) of electronic excitations as a function of time delay (via time dependence of T_{el} and T_{ph}). $v(\mathbf{q})$ is the Coulomb interaction and $\pi_{\alpha\alpha}$ is the current-current response function (photon self-energy) for the polarization direction α . Useful optical quantities such as optical absorption $\sigma(\omega; T_{el}, T_{ph}) = i\pi_{\alpha\alpha}(\mathbf{q} = 0, \omega)/\omega$ or photoconductivity $\Delta\sigma(\omega; T_{el}, T_{ph}) = \sigma(\omega; T_{el}, T_{ph}) - \sigma(\omega; T_{el} = T_{ph} = T_0)$ can also be simulated in the same way. The combination of Eq. (41) and the TTM equations was recently utilized in order to track ultrafast dynamics of Dirac plasmon in graphene, including energy loss of plasmon in non-equilibrium regime [68]. It was concluded that although steady state plasmon is mostly damped due to scatterings with acoustic phonons, the non-equilibrium Dirac plasmon dissipates most of its energy on intrinsic strongly coupled optical phonons. The same approach was also applied to study laser-induced band renormalizations close to van Hove singularity point of graphene band structure [205,206], where it was concluded that electron-phonon coupling plays a significant role in photo-induced band modifications in graphene [95].

Note that the approach of incorporating time dependence into Eqs. (40) and (41) via the TTM results is actually general and can be applied to any spectral function or self-energy defined in terms of electron and phonon distribution functions. For instance, this approach was exploited to monitor hot-phonon dynamics in conventional superconductor MgB_2 via phonon spectral function $B(\omega; T_{el}, T_{ph})$ and many-body phonon self-energy $\Pi(\omega; T_{el}, T_{ph})$ of strongly-coupled E_{2g} mode [80]. All in all, this way of modelling ultrafast carrier and lattice thermalization can provide many microscopic insights of spectroscopic quantities in time domain, and was proven to have a well-balanced ratio between accuracy and numerical cost.

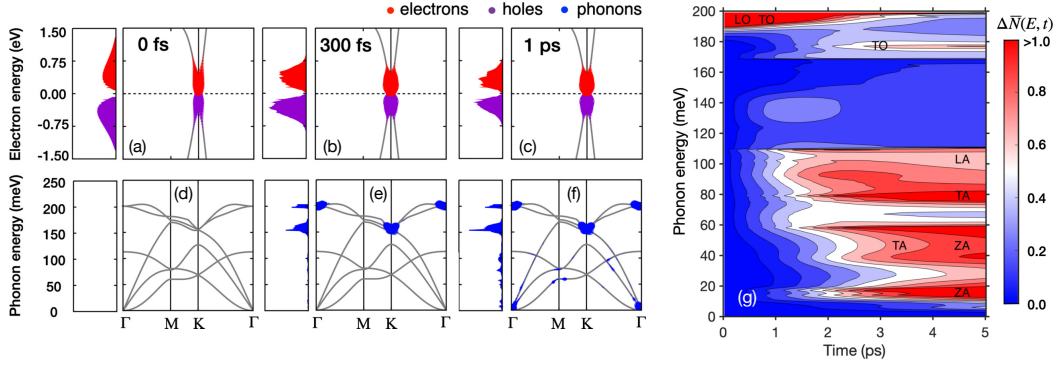


Figure 9. Population of excited electrons and holes for an initial electronic excitation (a) superimposed to the band structure of graphene, and at subsequent time steps throughout the non-equilibrium dynamics as obtained from the solution of the time-dependent Boltzmann equation (b-c). The left panels denote the density of states of electrons and holes. (d-f) Time-dependent phonon distribution functions $n_{\mathbf{q}\nu}(t)$ superimposed to the phonon dispersion for several time snapshot, with the point size being proportional to $n_{\mathbf{q}\nu}(t)$. (g) Energy resolved phonon population $n_{\mathbf{q}\nu}(t)$ as a function of time. Reproduced from Ref. [143].

4.3. Non-equilibrium lattice dynamics from the time-dependent Boltzmann equation

To illustrate the application of the TDBE formalism to the ultrafast electron-phonon dynamics of 2D materials and its suitability for the description of these phenomena, we report in Fig. 9 ultrafast dynamics simulations for graphene obtained from the numerical solutions of Eqs. (27) and (28) and reproduced from Ref. [143]. In panels (a)-(c), the electron ($f_{n\mathbf{k}}$) and hole ($1-f_{n\mathbf{k}}$) distribution functions are superimposed to the band dispersion of graphene for energies above and below the Fermi level (dashed) for several time delays. The initial ($t = 0$) distribution of electrons and holes loses its excess energy via emitting phonon in the vicinity of the Γ and K high symmetry points and relaxes back to Fermi level within few picoseconds. The non-equilibrium phonon population is illustrated in Figs. 9 (d)-(f), where the point size is proportional to the phonon occupation $n_{\mathbf{q}\nu}(t)$. The phonon population at 300 fs (Fig. 9 (e)) is characterized by an enhancement of the number LO and TO phonons at Γ and K, indicating that these modes constitute the primary decay path for excited electrons for the initial phases of the relaxation. These findings are compatible with the Eliashberg function shown in Fig. 7 (b). On longer time scales, the phonon-phonon scattering leads to the thermalization of lattice and a redistribution to the excess energy of these modes to low-energy modes Fig. 9 (g).

More generally, phonon-emission processes are constrained by energy and momentum conservation laws, which reduce the phase-space available for phonon-assisted electronic transitions. For example, graphene carriers in the vicinity of the Fermi level at K can scatter to states within the same Dirac cone at K, leading to the emission of phonons with $\mathbf{q} \simeq \Gamma$, alternatively they can scatter to the second Dirac cone at $-\text{K}$, emitting phonons with crystal momentum around K or $-\text{K}$. Transitions to other region of the BZ are forbidden as they violate conservation laws. This stringent momentum selectivity confines the emitted phonons to narrow regions in reciprocal space, leading to the emergence of *hot spots* in the BZ, i.e., regions characterized by an enhanced vibrational temperature. Figure 10 (a) illustrates the BZ and high-symmetry points of monolayer MoS_2 , reproduced from Ref. [207]. The superimposed color coding denotes the effective vibrational temperature obtained by inverting the Bose-Einstein distribu-

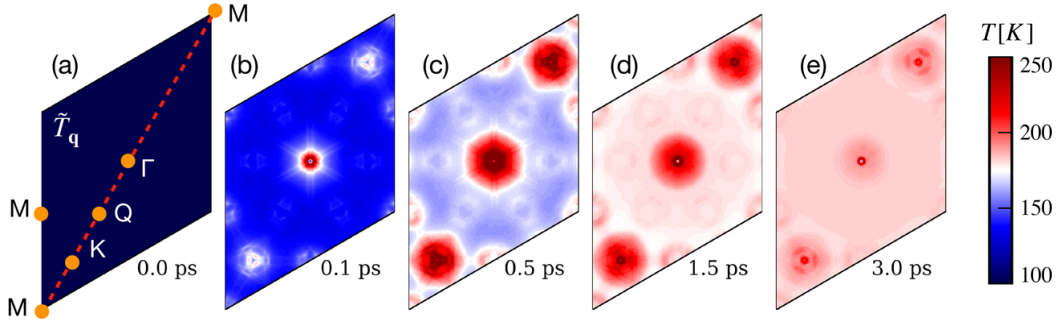


Figure 10. (a) Hexagonal Brillouin zone and high-symmetry points (dots) of monolayer MoS₂. The color coding reflects the effective vibrational temperature of the lattice for an initial ($t = 0$) state of thermal equilibrium at $T = 100$ K (see color bar). (b-e) Enhancement of the phonon temperature in the vicinity of the Γ and K high-symmetry points due to momentum-selective phonon emission throughout the relaxation of a photo-excited electronic distribution. Reproduced from Ref. [207].

tion as $T_{\mathbf{q}\nu}(t) = \hbar\omega_{\mathbf{q}\nu} \{k_B \ln[1 + n_{\mathbf{q}\nu}(t)]\}^{-1}$, and averaging over all mode indices ν via $\tilde{T}_{\mathbf{q}} = N_{\text{ph}}^{-1} \sum_{\nu} T_{\mathbf{q}\nu}$ - with $N_{\text{ph}} = 9$ being the number of phonons of monolayer MoS₂. Here, the phonon distribution function $n_{\mathbf{q}\nu}(t)$ is obtained from the solution of the coupled TDBE for electrons and lattice. The preferential emission of phonons around Γ , K, and $-K$ is reflected by the enhanced vibrational temperature at these high-symmetry points for the initial phases of hot-carrier relaxation. Phonon hot-spots in the BZ can persist for several picoseconds, until the onset of phonon-phonon scattering processes restores a regime of thermal equilibrium.

5. Summary and Outlook

In this manuscript we introduced parameter-free theoretical approaches for the study of the coupled ultrafast dynamics of electrons and phonons in solids, and we reviewed their application to the prototypical two-dimensional materials, such as graphene and MoS₂.

The two-temperature and the non-thermal lattice models recast the thermalization dynamics of electrons and phonons into a set of coupled first-order differential equations, which is formally equivalent to the one governing the temperature evolution of coupled thermal baths. While on the one hand these approximations are sufficient to capture the characteristic timescales and dynamics of the electron thermalization with the lattice revealed by pump-probe experiments, on the other hand, the non-equilibrium electron, vibrational and structural dynamics are poorly described, restricting the domain of applicability of these approaches. In particular, the emergence of non-equilibrium states of the lattice often entails phonon populations characterized by strong anisotropy in the Brillouin zone that cannot be captured by a Bose-Einstein function.

The time-dependent Boltzmann equation overcomes these limitations. As compared to models, the advantage of this approach is two-fold: (i) it provides a description of ultrafast electron and phonon dynamics with full momentum resolution (ii) it accounts for phase-space constraints in phonon-assisted electronic transitions. These points are important prerequisites to capture the emergence of phonon hot-spots in the Brillouin zone, which have recently been revealed by ultrafast diffuse scattering experiments [38,39,83,145,152]. Additionally, the collision integrals can be made fully parameter-

free by determining electron-phonon and phonon-phonon coupling matrix elements via available first-principles electronic-structure codes [138,157,208].

Fostered by the relentless advances in the experimental characterization of ultrafast phenomena, first-principles approaches for coupled electron-phonon dynamics constitute a rapidly evolving research field. Many non-equilibrium phenomena, however, still represent *de facto* a challenge for ab-initio techniques. These include, for instance, coherence and dephasing of electronic and vibrational excitations [209], correlation effects on the electron dynamics [210], structural phase transitions [211–213], topological Floquet states [214], and the transient formation of quasiparticle states [215]. The development of accurate and efficient first-principles techniques capable of tackling these phenomena remains a key research priority in the field of ultrafast science. In this respect, approaches based on the density-matrix formalism [194] and non-equilibrium Green’s functions [210] are promising routes to overcome the inherent limitations of the Boltzmann equation: recent studies explored new directions to reduce the notoriously high computational cost of NEGF methods [216] paving the way towards a rigorous quantum mechanical description of coherent and correlated dynamical phenomena in condensed matter [217].

Acknowledgement(s)

This project has been funded by the Deutsche Forschungsgemeinschaft (DFG) – Projektnummer 443988403. D.N. acknowledges financial support from the Croatian Science Foundation (Grant no. UIP-2019-04-6869) and from the European Regional Development Fund for the “Center of Excellence for Advanced Materials and Sensing Devices” (Grant No. KK.01.1.1.01.0001).

Appendix A. Analytical solution of the TTM

Below we report the analytical solution of the TTM for the limiting case of temperature-independent heat capacities. The TTM equations in absence of external driving field are reported below:

$$\frac{\partial T_{\text{ph}}}{\partial t} = \frac{g}{C_{\text{ph}}}(T_{\text{el}} - T_{\text{ph}}) \quad , \quad (42)$$

$$\frac{\partial T_{\text{el}}}{\partial t} = \frac{g}{C_{\text{el}}}(T_{\text{ph}} - T_{\text{el}}) \quad . \quad (43)$$

The TTM thus forms a set of two coupled first-order differential equation, which can be solved analytically via standard techniques. Its solution is:

$$T_{\text{el}}(t) = a_1 e^{-\gamma t} + a_2 \quad , \quad (44)$$

$$T_{\text{ph}}(t) = -\frac{C_{\text{el}} a_1}{C_{\text{ph}}} e^{-\gamma t} + a_2 \quad , \quad (45)$$

where we introduced the constants $a_1 = (T_{\text{el}}^0 - T_{\text{ph}}^0)C_{\text{ph}}/(C_{\text{ph}} + C_{\text{el}})$, $a_2 = T_{\text{el}}^0 - c_1$, and $\gamma = g/(1/C_{\text{el}} + 1/C_{\text{ph}})$. The solution is easily verified by substitution.

By introducing a source term coupled to the electronic temperature, the TTM gets

modified as follows:

$$\frac{\partial T_{\text{el}}}{\partial t} = \frac{g}{C_{\text{el}}}(T_{\text{ph}} - T_{\text{el}}) + S(t) \quad , \quad (46)$$

where $S(t)$ describes the interaction with a light pulse, and the second equation remains unchanged. Analytic solution of the TTM is still possible for a simple time dependence of $S(t)$. For example, by considering $S(t) = \alpha e^{-\frac{t}{\tau}} \theta(t)$, the solution can be written as:

$$T_{\text{el}}(t) = -\tau b_1 e^{-\frac{t}{\tau}} - b_2 \gamma^{-1} e^{-\gamma t} + b_3 \quad , \quad (47)$$

$$T_{\text{ph}}(t) = T_{\text{el}}(t) + \frac{C_{\text{el}}}{g} \left[(b_1 - \alpha) e^{-\frac{t}{\tau}} + b_2 e^{-\gamma t} \right] \quad , \quad (48)$$

with the constants:

$$b_1 = \alpha \left(\frac{g\tau}{C_{\text{ph}}} - 1 \right) (\gamma\tau - 1)^{-1} \quad , \quad (49)$$

$$b_2 = \frac{g}{C_{\text{el}}}(T_{\text{ph}}^0 - T_{\text{el}}^0) + \alpha - b_1 \quad , \quad (50)$$

$$b_3 = T_{\text{el}}^0 + \frac{b_2}{\gamma} + b_1 \tau \quad . \quad (51)$$

References

- [1] Feliciano Giustino. Electron-phonon interactions from first principles. *Rev. Mod. Phys.*, 89:015003, Feb 2017.
- [2] P B Allen and V Heine. Theory of the temperature dependence of electronic band structures. *Journal of Physics C: Solid State Physics*, 9(12):2305–2312, jun 1976.
- [3] P. B. Allen and M. Cardona. Theory of the temperature dependence of the direct gap of germanium. *Phys. Rev. B*, 23:1495–1505, Feb 1981.
- [4] Feliciano Giustino, Steven G. Louie, and Marvin L. Cohen. Electron-phonon renormalization of the direct band gap of diamond. *Phys. Rev. Lett.*, 105:265501, Dec 2010.
- [5] Samuel Poncé, Elena R. Margine, and Feliciano Giustino. Towards predictive many-body calculations of phonon-limited carrier mobilities in semiconductors. *Phys. Rev. B*, 97:121201, Mar 2018.
- [6] P. B. Allen. Electron-phonon effects in the infrared properties of metals. *Phys. Rev. B*, 3:305, Jan 1971.
- [7] Cheol-Hwan Park, Nicola Bonini, Thibault Sohier, Georgy Samsonidze, Boris Kozinsky, Matteo Calandra, Francesco Mauri, and Nicola Marzari. Electron–phonon interactions and the intrinsic electrical resistivity of graphene. *Nano Letters*, 14(3):1113, 2014.
- [8] Samuel Poncé, Wenbin Li, Sven Reichardt, and Feliciano Giustino. First-principles calculations of charge carrier mobility and conductivity in bulk semiconductors and two-dimensional materials. *Reports on Progress in Physics*, 83(3):036501, feb 2020.
- [9] Emmanouil Kioupakis, Patrick Rinke, André Schleife, Friedhelm Bechstedt, and Chris G. Van de Walle. Free-carrier absorption in nitrides from first principles. *Phys. Rev. B*, 81:241201, Jun 2010.
- [10] Jesse Noffsinger, Emmanouil Kioupakis, Chris G. Van de Walle, Steven G. Louie, and Marvin L. Cohen. Phonon-assisted optical absorption in silicon from first principles. *Phys. Rev. Lett.*, 108:167402, Apr 2012.
- [11] Ana M. Brown, Ravishankar Sundararaman, Prineha Narang, William A. Goddard, and

- Harry A. Atwater. Nonradiative plasmon decay and hot carrier dynamics: Effects of phonons, surfaces, and geometry. *ACS Nano*, 10(1):957, 2016.
- [12] Dino Novko. Dopant-induced plasmon decay in graphene. *Nano Letters*, 17(11):6991, 2017.
- [13] Fabio Caruso, Dino Novko, and Claudia Draxl. Phonon-assisted damping of plasmons in three- and two-dimensional metals. *Phys. Rev. B*, 97:205118, May 2018.
- [14] S. Piscanec, M. Lazzeri, Francesco Mauri, A. C. Ferrari, and J. Robertson. Kohn anomalies and electron-phonon interactions in graphite. *Phys. Rev. Lett.*, 93:185503, Oct 2004.
- [15] Michele Lazzeri and Francesco Mauri. Nonadiabatic kohn anomaly in a doped graphene monolayer. *Phys. Rev. Lett.*, 97:266407, Dec 2006.
- [16] Matteo Calandra, Gianni Profeta, and Francesco Mauri. Adiabatic and nonadiabatic phonon dispersion in a wannier function approach. *Phys. Rev. B*, 82:165111, Oct 2010.
- [17] Fabio Caruso, Moritz Hoesch, Philipp Achatz, Jorge Serrano, Michael Krisch, Etienne Bustarret, and Feliciano Giustino. Nonadiabatic kohn anomaly in heavily boron-doped diamond. *Phys. Rev. Lett.*, 119:017001, Jul 2017.
- [18] Dino Novko. Nonadiabatic coupling effects in mgB_2 reexamined. *Phys. Rev. B*, 98:041112, 2018.
- [19] Peio Garcia-Goiricelaya, Jon Lafuente-Bartolome, Idoia G. Gurtubay, and Asier Eiguren. Emergence of large nonadiabatic effects induced by the electron-phonon interaction on the complex vibrational quasiparticle spectrum of doped monolayer mos_2 . *Phys. Rev. B*, 101:054304, Feb 2020.
- [20] Dino Novko. Broken adiabaticity induced by lifshitz transition in MoS_2 and WS_2 single layers. *Communications Physics*, 3(1), feb 2020.
- [21] C. Verdi, F. Caruso, and F. Giustino. Origin of the crossover from polarons to Fermi liquids in transition metal oxides. *Nat. Commun.*, 8:15769, 2017.
- [22] J. M. Riley, F. Caruso, C. Verdi, L. B. Duffy, M. D. Watson, L. Bawden, K. Volckaert, G. van der Laan, T. Hesjedal, M. Hoesch, F. Giustino, and P. D. C. King. Crossover from lattice to plasmonic polarons of a spin-polarised electron gas in ferromagnetic euo. *Nature Comm.*, 9:2305, 2018.
- [23] Fabio Caruso, Carla Verdi, Samuel Poncé, and Feliciano Giustino. Electron-plasmon and electron-phonon satellites in the angle-resolved photoelectron spectra of n -doped anatase tio_2 . *Phys. Rev. B*, 97:165113, Apr 2018.
- [24] Mingu Kang, Sung Won Jung, Woo Jong Shin, Yeongsup Sohn, Sae Hee Ryu, Timur K. Kim, Moritz Hoesch, and Keun Su Kim. Holstein polaron in a valley-degenerate two-dimensional semiconductor. *Nature Mater.*, 17(8):676, 2018.
- [25] Peio Garcia-Goiricelaya, Jon Lafuente-Bartolome, Idoia G. Gurtubay, and Asier Eiguren. Long-living carriers in a strong electron-phonon interacting two-dimensional doped semiconductor. *Commun. Phys.*, 2(1):81, 2019.
- [26] J. P. Carbotte and F. Marsiglio. *Electron-Phonon Superconductivity*, page 233. Springer Berlin Heidelberg, Berlin, Heidelberg, 2003.
- [27] M. Lüders, M. A. L. Marques, N. N. Lathiotakis, A. Floris, G. Profeta, L. Fast, A. Continenza, S. Massidda, and E. K. U. Gross. Ab initio theory of superconductivity. i. density functional formalism and approximate functionals. *Phys. Rev. B*, 72:024545, Jul 2005.
- [28] M. A. L. Marques, M. Lüders, N. N. Lathiotakis, G. Profeta, A. Floris, L. Fast, A. Continenza, E. K. U. Gross, and S. Massidda. Ab initio theory of superconductivity. ii. application to elemental metals. *Phys. Rev. B*, 72:024546, Jul 2005.
- [29] E. R. Margine and F. Giustino. Anisotropic migdal-eliasberg theory using wannier functions. *Phys. Rev. B*, 87:024505, Jan 2013.
- [30] Matteo Calandra, I. I. Mazin, and Francesco Mauri. Effect of dimensionality on the charge-density wave in few-layer $2H\text{-NbSe}_2$. *Phys. Rev. B*, 80:241108, Dec 2009.
- [31] K Rossnagel. On the origin of charge-density waves in select layered transition-metal dichalcogenides. *Journal of Physics: Condensed Matter*, 23(21):213001, may 2011.
- [32] Xuetao Zhu, Yanwei Cao, Jiandi Zhang, E. W. Plummer, and Jiandong Guo. Classification of charge density waves based on their nature. *Proceedings of the National Academy*

- of Sciences*, 112(8):2367, 2015.
- [33] Marco Bernardi, Derek Vigil-Fowler, Johannes Lischner, Jeffrey B. Neaton, and Steven G. Louie. Ab initio study of hot carriers in the first picosecond after sunlight absorption in silicon. *Phys. Rev. Lett.*, 112:257402, Jun 2014.
 - [34] M. Lisowski, P.A. Loukakos, U. Bovensiepen, J. Stähler, C. Gahl, and M. Wolf. Ultra-fast dynamics of electron thermalization, cooling and transport effects in Ru(001). *Applied Physics A: Materials Science & Processing*, 78(2):165–176, January 2004.
 - [35] Alberto de la Torre, Dante M. Kennes, Martin Claassen, Simon Gerber, James W. McIver, and Michael A. Sentef. Colloquium: Nonthermal pathways to ultrafast control in quantum materials. *Rev. Mod. Phys.*, 93:041002, Oct 2021.
 - [36] U. Bovensiepen and P.S. Kirchmann. Elementary relaxation processes investigated by femtosecond photoelectron spectroscopy of two-dimensional materials. *Laser & Photonics Reviews*, 6(5):589, 2012.
 - [37] G. Rohde, A. Stange, A. Müller, M. Behrendt, L.-P. Oloff, K. Hanff, T.-J. Albert, P. Hein, K. Rossnagel, and M. Bauer. Ultrafast Formation of a Fermi-Dirac Distributed Electron Gas. *Phys. Rev. Lett.*, 121(25):256401, December 2018.
 - [38] Lutz Waldecker, Roman Bertoni, Ralph Ernstorfer, and Jan Vorberger. Electron-Phonon Coupling and Energy Flow in a Simple Metal beyond the Two-Temperature Approximation. *Phys. Rev. X*, 6(2):021003, April 2016. 00000.
 - [39] Mark J. Stern, Laurent P. René de Cotret, Martin R. Otto, Robert P. Chatelain, Jean-Philippe Boisvert, Mark Sutton, and Bradley J. Siwick. Mapping momentum-dependent electron-phonon coupling and nonequilibrium phonon dynamics with ultrafast electron diffuse scattering. *Phys. Rev. B*, 97:165416, Apr 2018.
 - [40] H.A. Dürr, R. Ernstorfer, and B.J. Siwick. Revealing momentum-dependent electron-phonon and phonon-phonon coupling in complex materials with ultrafast electron diffuse scattering. *MRS Bulletin*, 46:731, 2021.
 - [41] M.I. Kaganov, I.M. Lifshitz, and L.V. Tanatarov. Electron emission from metal surfaces exposed to ultrashort laser pulses. *Sov. Phys. JETP*, 4(2):173, 1957.
 - [42] I.M. Lifshits, M.I. Kaganov, and L.V. Tanatarov. On the theory of the changes produced in metals by radiation. *The Soviet Journal of Atomic Energy*, 6(4):261, 1960.
 - [43] S. I. Anisimov, B. L. Kapeliovich, and T. L. Perel'man. Electron emission from metal surfaces exposed to ultrashort laser pulses. *Sov. Phys. JETP*, 39(2):375, 1973.
 - [44] Philip B. Allen. Theory of thermal relaxation of electrons in metals. *Phys. Rev. Lett.*, 59:1460–1463, Sep 1987.
 - [45] P. B. Corkum, F. Brunel, N. K. Sherman, and T. Srinivasan-Rao. Thermal Response of Metals to Ultrashort-Pulse Laser Excitation. *Physical Review Letters*, 61(25):2886–2889, December 1988. 00000.
 - [46] S. D. Brorson, A. Kazeroonian, J. S. Moodera, D. W. Face, T. K. Cheng, E. P. Ippen, M. S. Dresselhaus, and G. Dresselhaus. Femtosecond room-temperature measurement of the electron-phonon coupling constant γ in metallic superconductors. *Physical Review Letters*, 64(18):2172–2175, April 1990. 00779.
 - [47] B. Rethfeld, A. Kaiser, M. Vicanek, and G. Simon. Ultrafast dynamics of nonequilibrium electrons in metals under femtosecond laser irradiation. *Phys. Rev. B*, 65(21):214303, May 2002. 00511.
 - [48] Lan Jiang and Hai-Lung Tsai. Improved Two-Temperature Model and Its Application in Ultrashort Laser Heating of Metal Films. *Journal of Heat Transfer*, 127(10):1167–1173, October 2005. 00284.
 - [49] E. Carpene. Ultrafast laser irradiation of metals: Beyond the two-temperature model. *Physical Review B*, 74(2):024301, July 2006. 00000.
 - [50] Zhibin Lin, Leonid V. Zhigilei, and Vittorio Celli. Electron-phonon coupling and electron heat capacity of metals under conditions of strong electron-phonon nonequilibrium. *Physical Review B*, 77(7):075133, February 2008. 01239.
 - [51] Matteo Conforti and Giuseppe Della Valle. Derivation of third-order nonlinear susceptibility of thin metal films as a delayed optical response. *Physical Review B*, 85(24):245423,

June 2012. 00000.

- [52] B. Y. Mueller and B. Rethfeld. Relaxation dynamics in laser-excited metals under nonequilibrium conditions. *Physical Review B*, 87(3):035139, January 2013. 00220.
- [53] R. B. Wilson, Joseph P. Feser, Gregory T. Hohensee, and David G. Cahill. Two-channel model for nonequilibrium thermal transport in pump-probe experiments. *Physical Review B*, 88(14):144305, October 2013. 00000.
- [54] Taeho Shin, Samuel W. Teitelbaum, Johanna Wolfson, Maria Kandyla, and Keith A. Nelson. Extended two-temperature model for ultrafast thermal response of band gap materials upon impulsive optical excitation. *The Journal of Chemical Physics*, 143(19):194705, November 2015. 00000.
- [55] Ana M. Brown, Ravishankar Sundararaman, Prineha Narang, William A. Goddard, and Harry A. Atwater. *Ab initio* phonon coupling and optical response of hot electrons in plasmonic metals. *Physical Review B*, 94(7):075120, August 2016. 00000.
- [56] Ivor Lončarić, M. Alducin, P. Saalfrank, and J. I. Juaristi. Femtosecond-laser-driven molecular dynamics on surfaces: Photodesorption of molecular oxygen from ag(110). *Phys. Rev. B*, 93:014301, Jan 2016.
- [57] Da-Quan Xian and Xiao-Hong Li. An analytic study on the two-temperature model for electron-lattice thermal dynamic process. *Therm sci*, 21(4):1777–1782, 2017. 00002.
- [58] Meng An, Qichen Song, Xiaoxiang Yu, Han Meng, Dengke Ma, Ruiyang Li, Zelin Jin, Baoling Huang, and Nuo Yang. Generalized Two-Temperature Model for Coupled Phonons in Nanosized Graphene. *Nano Letters*, 17(9):5805–5810, September 2017. 00000.
- [59] Sridhar Sadasivam, Maria K. Y. Chan, and Pierre Darancet. Theory of thermal relaxation of electrons in semiconductors. *Phys. Rev. Lett.*, 119:136602, Sep 2017.
- [60] Pablo Maldonado, Karel Carva, Martina Flammer, and Peter M. Oppeneer. Theory of out-of-equilibrium ultrafast relaxation dynamics in metals. *Physical Review B*, 96(17):174439, November 2017. 00000.
- [61] P. Maldonado, T. Chase, A. H. Reid, X. Shen, R. K. Li, K. Carva, T. Payer, M. Horn von Hoegen, K. Sokolowski-Tinten, X. J. Wang, P. M. Oppeneer, and H. A. Dürr. Tracking the ultrafast nonequilibrium energy flow between electronic and lattice degrees of freedom in crystalline nickel. *Phys. Rev. B*, 101(10):100302, March 2020. 00015.
- [62] D. Novko, J.-C. Tremblay, M. Alducin, and J.-I. Juaristi. Ultrafast Transient Dynamics of Adsorbates on Surfaces Deciphered: The Case of CO on Cu(100). *Physical Review Letters*, 122(1):016806, January 2019. 00000.
- [63] N. A. Smirnov. Copper, gold, and platinum under femtosecond irradiation: Results of first-principles calculations. *Physical Review B*, 101(9):094103, March 2020. 00006.
- [64] Sarah B. Naldo, Andrius V. Bernotas, and Brian F. Donovan. Understanding the sensitivity of the two-temperature model for electron–phonon coupling measurements. *Journal of Applied Physics*, 128(8):085102, August 2020. 00000.
- [65] P. Di Pietro, N. Adhlakha, F. Piccirilli, A. Di Gaspare, J. Moon, S. Oh, S. Di Mitri, S. Spampinati, A. Perucchi, and S. Lupi. Terahertz tuning of dirac plasmons in bi₂se₃ topological insulator. *Phys. Rev. Lett.*, 124:226403, Jun 2020.
- [66] Ulrike Ritzmann, Peter M. Oppeneer, and Pablo Maldonado. Theory of out-of-equilibrium electron and phonon dynamics in metals after femtosecond laser excitation. *Physical Review B*, 102(21):214305, December 2020. 00002.
- [67] Wuli Miao and Moran Wang. Nonequilibrium effects on the electron-phonon coupling constant in metals. *Phys. Rev. B*, 103(12):125412, March 2021. 00001.
- [68] Dino Novko. First-principles study of ultrafast dynamics of Dirac plasmon in graphene. *New Journal of Physics*, 23(4):043023, April 2021. 00001.
- [69] T. P. H. Sidiropoulos, N. Di Palo, D. E. Rivas, S. Severino, M. Reduzzi, B. Nandy, B. Bauerhenne, S. Krylow, T. Vasileiadis, T. Danz, P. Elliott, S. Sharma, K. Dewhurst, C. Ropers, Y. Joly, K. M. E. Garcia, M. Wolf, R. Ernstorfer, and J. Biegert. Probing the energy conversion pathways between light, carriers, and lattice in real time with attosecond core-level spectroscopy. *Phys. Rev. X*, 11:041060, Dec 2021.

- [70] J. G. Fujimoto, J. M. Liu, E. P. Ippen, and N. Bloembergen. Femtosecond Laser Interaction with Metallic Tungsten and Nonequilibrium Electron and Lattice Temperatures. *Physical Review Letters*, 53(19):1837–1840, November 1984. 00658.
- [71] W. S. Fann, R. Storz, H. W. K. Tom, and J. Bokor. Direct measurement of nonequilibrium electron-energy distributions in subpicosecond laser-heated gold films. *Physical Review Letters*, 68(18):2834–2837, May 1992. 00000.
- [72] W. S. Fann, R. Storz, H. W. K. Tom, and J. Bokor. Electron thermalization in gold. *Physical Review B*, 46(20):13592–13595, November 1992. 00000.
- [73] T. Hertel, E. Knoesel, M. Wolf, and G. Ertl. Ultrafast Electron Dynamics at Cu(111): Response of an Electron Gas to Optical Excitation. *Physical Review Letters*, 76(3):535–538, January 1996. 00455.
- [74] L. Perfetti, P. A. Loukakos, M. Lisowski, U. Bovensiepen, H. Eisaki, and M. Wolf. Ultrafast electron relaxation in superconducting $\text{Bi}_2\text{Sr}_2\text{CaCu}_2\text{O}_{8+\delta}$ by time-resolved photoelectron spectroscopy. *Phys. Rev. Lett.*, 99:197001, Nov 2007.
- [75] Mischa Bonn, Daniel N. Denzler, Stephan Funk, Martin Wolf, S.-Svante Wellershoff, and Julius Hohlfeld. Ultrafast electron dynamics at metal surfaces: Competition between electron-phonon coupling and hot-electron transport. *Physical Review B*, 61(2):1101–1105, January 2000. 00000.
- [76] Jens Christian Johannsen, Søren Ulstrup, Federico Cilento, Alberto Crepaldi, Michele Zacchigna, Cephise Cacho, I. C. Edmond Turcu, Emma Springate, Felix Fromm, Christian Raidel, Thomas Seyller, Fulvio Parmigiani, Marco Grioni, and Philip Hofmann. Direct View of Hot Carrier Dynamics in Graphene. *Phys. Rev. Lett.*, 111(2):027403, July 2013.
- [77] Isabella Gierz, Jesse C. Petersen, Matteo Mitrano, Cephise Cacho, I. C. Edmond Turcu, Emma Springate, Alexander Stöhr, Axel Köhler, Ulrich Starke, and Andrea Cavalleri. Snapshots of non-equilibrium Dirac carrier distributions in graphene. *Nature Mater*, 12(12):1119–1124, December 2013.
- [78] Jih-An Yang, Stephen Parham, Daniel Dessau, and Dmitry Reznik. Novel Electron-Phonon Relaxation Pathway in Graphite Revealed by Time-Resolved Raman Scattering and Angle-Resolved Photoemission Spectroscopy. *Sci. Rep.*, 7:40876, 2017.
- [79] Fabio Caruso, Dino Novko, and Claudia Draxl. Photoemission signatures of nonequilibrium carrier dynamics from first principles. *Phys. Rev. B*, 101(3):035128, January 2020. 00012.
- [80] Dino Novko, Fabio Caruso, Claudia Draxl, and Emmanuele Cappelluti. Ultrafast Hot Phonon Dynamics in MgB₂ Driven by Anisotropic Electron-Phonon Coupling. *Phys. Rev. Lett.*, 124(7):077001, February 2020. 00005.
- [81] N. Pellatz, S. Roy, J-W. Lee, J. L. Schad, H. Kandel, N. Arndt, C. B. Eom, A. F. Kemper, and D. Reznik. Relaxation timescales and electron-phonon coupling in optically pumped $\text{YBa}_2\text{Cu}_3\text{O}_{6+x}$ revealed by time-resolved raman scattering. *Phys. Rev. B*, 104:L180505, Nov 2021.
- [82] T. Chase, M. Trigo, A. H. Reid, R. Li, T. Vecchione, X. Shen, S. Weathersby, R. Coffee, N. Hartmann, D. A. Reis, X. J. Wang, and H. A. Dürr. Ultrafast electron diffraction from non-equilibrium phonons in femtosecond laser heated Au films. *Applied Physics Letters*, 108(4):041909, January 2016. 00000.
- [83] Laurent P. René de Cotret, Jan-Hendrik Pöhls, Mark J. Stern, Martin R. Otto, Mark Sutton, and Bradley J. Siwick. Time- and momentum-resolved phonon population dynamics with ultrafast electron diffuse scattering. *Phys. Rev. B*, 100(21):214115, December 2019. 00000.
- [84] H. E. Elsayed-Ali, T. B. Norris, M. A. Pessot, and G. A. Mourou. Time-resolved observation of electron-phonon relaxation in copper. *Physical Review Letters*, 58(12):1212–1215, March 1987. 00772.
- [85] R. W. Schoenlein, W. Z. Lin, J. G. Fujimoto, and G. L. Eesley. Femtosecond studies of nonequilibrium electronic processes in metals. *Physical Review Letters*, 58(16):1680–1683, April 1987. 00847.

- [86] Rogier H. M. Groeneveld, Rudolf Sprik, and Ad Lagendijk. Effect of a nonthermal electron distribution on the electron-phonon energy relaxation process in noble metals. *Physical Review B*, 45(9):5079–5082, March 1992. 00203.
- [87] T. Juhasz, H. E. Elsayed-Ali, G. O. Smith, C. Suárez, and W. E. Bron. Direct measurements of the transport of nonequilibrium electrons in gold films with different crystal structures. *Physical Review B*, 48(20):15488–15491, November 1993. 00000.
- [88] C.-K. Sun, F. Vallée, L. H. Acioli, E. P. Ippen, and J. G. Fujimoto. Femtosecond-tunable measurement of electron thermalization in gold. *Physical Review B*, 50(20):15337–15348, November 1994. 00853.
- [89] J. Hohlfeld, J.G. Müller, S.-S. Wellershoff, and E. Matthias. Time-resolved thermoreflectivity of thin gold films and its dependence on film thickness. *Applied Physics B: Lasers and Optics*, 64(3):387–390, March 1997. 00000.
- [90] S.-S. Wellershoff, J. Hohlfeld, J. Gütde, and E. Matthias. The role of electron-phonon coupling in femtosecond laser damage of metals. *Applied Physics A Materials Science & Processing*, 69(S1):S99–S107, December 1999. 00542.
- [91] J. Hohlfeld, S.-S. Wellershoff, J. Gütde, U. Conrad, V. Jähnke, and E. Matthias. Electron and lattice dynamics following optical excitation of metals. *Chemical Physics*, 251(1-3):237–258, January 2000. 00954.
- [92] Muneaki Hase, Kunie Ishioka, Jure Demsar, Kiminori Ushida, and Masahiro Kitajima. Ultrafast dynamics of coherent optical phonons and nonequilibrium electrons in transition metals. *Phys. Rev. B*, 71(18):184301, May 2005.
- [93] G. Della Valle, M. Conforti, S. Longhi, G. Cerullo, and D. Brida. Real-time optical mapping of the dynamics of nonthermal electrons in thin gold films. *Physical Review B*, 86(15):155139, October 2012. 00000.
- [94] Michele Ortolani, Andrea Mancini, Arne Budweg, Denis Garoli, Daniele Brida, and Francesco de Angelis. Pump-probe spectroscopy study of ultrafast temperature dynamics in nanoporous gold. *Physical Review B*, 99(3):035435, January 2019. 00000.
- [95] Dino Novko and Marko Kralj. Phonon-assisted processes in the ultraviolet-transient optical response of graphene. *NPJ 2D Mater. Appl.*, 3:48, 2019.
- [96] P. Bresson, J-F. Bryche, M. Besbes, J. Moreau, P-L. Karsenti, P. G. Charette, D. Morris, and M. Canva. Improved two-temperature modeling of ultrafast thermal and optical phenomena in continuous and nanostructured metal films. *Physical Review B*, 102(15):155127, October 2020. 00000.
- [97] Manuel Obergfell and Jure Demsar. Tracking the time evolution of the electron distribution function in copper by femtosecond broadband optical spectroscopy. *Phys. Rev. Lett.*, 124:037401, Jan 2020.
- [98] Christopher C. S. Chan, Kezhou Fan, Han Wang, Zhanfeng Huang, Dino Novko, Keyou Yan, Jianbin Xu, Wallace C. H. Choy, Ivor Lončarić, and Kam Sing Wong. Uncovering the Electron-Phonon Interplay and Dynamical Energy-Dissipation Mechanisms of Hot Carriers in Hybrid Lead Halide Perovskites. *Adv. Energy Mater.*, 11:2003071, 2021.
- [99] Hung-Tzu Chang, Alexander Guggenmos, Scott K. Cushing, Yang Cui, Naseem Ud Din, Shree Ram Acharya, Ilana J. Porter, Ulf Kleineberg, Volodymyr Turkowski, Talat S. Rahman, Daniel M. Neumark, and Stephen R. Leone. Electron thermalization and relaxation in laser-heated nickel by few-femtosecond core-level transient absorption spectroscopy. *Physical Review B*, 103(6):064305, February 2021. 00001.
- [100] Jau Tang. Coherent phonon excitation and linear thermal expansion in structural dynamics and ultrafast electron diffraction of laser-heated metals. *The Journal of Chemical Physics*, 128(16):164702, April 2008. 00000.
- [101] Y. Giret, A. Gellé, and B. Arnaud. Entropy Driven Atomic Motion in Laser-Excited Bismuth. *Physical Review Letters*, 106(15):155503, April 2011. 00000.
- [102] B. Holst, V. Recoules, S. Mazevet, M. Torrent, A. Ng, Z. Chen, S. E. Kirkwood, V. Sameoglu, M. Reid, and Y. Y. Tsui. *Ab initio* model of optical properties of two-temperature warm dense matter. *Physical Review B*, 90(3):035121, July 2014. 00000.
- [103] P. M. Leguay, A. Lévy, B. Chimier, F. Deneuille, D. Descamps, C. Fourment, C. Goyon,

- S. Hulin, S. Petit, O. Peyrusse, J. J. Santos, P. Combis, B. Holst, V. Recoules, P. Renaudin, L. Videau, and F. Dorchies. Ultrafast Short-Range Disordering of Femtosecond-Laser-Heated Warm Dense Aluminum. *Physical Review Letters*, 111(24):245004, December 2013. 00000.
- [104] G. M. Petrov, A. Davidson, D. Gordon, and J. Peñano. Modeling of short-pulse laser-metal interactions in the warm dense matter regime using the two-temperature model. *Physical Review E*, 103(3):033204, March 2021. 00000.
- [105] Jacopo Simoni and Jérôme Daligault. First-Principles Determination of Electron-Ion Couplings in the Warm Dense Matter Regime. *Physical Review Letters*, 122(20):205001, May 2019. 00000.
- [106] O. Benhayoun, P.N. Terekhin, D.S. Ivanov, B. Rethfeld, and M.E. Garcia. Theory for heating of metals assisted by surface plasmon polaritons. *Applied Surface Science*, 569:150427, 2021.
- [107] E. Beaurepaire, J.-C. Merle, A. Daunois, and J.-Y. Bigot. Ultrafast Spin Dynamics in Ferromagnetic Nickel. *Physical Review Letters*, 76(22):4250–4253, May 1996. 00000.
- [108] D. J. Sanders and D. Walton. Effect of magnon-phonon thermal relaxation on heat transport by magnons. *Physical Review B*, 15(3):1489–1494, February 1977. 00000.
- [109] Michael Schreier, Akashdeep Kamra, Mathias Weiler, Jiang Xiao, Gerrit E. W. Bauer, Rudolf Gross, and Sebastian T. B. Goennenwein. Magnon, phonon, and electron temperature profiles and the spin Seebeck effect in magnetic insulator/normal metal hybrid structures. *Physical Review B*, 88(9):094410, September 2013. 00000.
- [110] M. Agrawal, V. I. Vasyuchka, A. A. Serga, A. D. Karenowska, G. A. Melkov, and B. Hillebrands. Direct Measurement of Magnon Temperature: New Insight into Magnon-Phonon Coupling in Magnetic Insulators. *Physical Review Letters*, 111(10):107204, September 2013. 00000.
- [111] Matteo Montagnese, Marian Otter, Xenophon Zotos, Dmitry A. Fishman, Nikolai Hlubek, Oleg Mityashkin, Christian Hess, Romuald Saint-Martin, Surjeet Singh, Alexandre Revcolevschi, and Paul H. M. van Loosdrecht. Phonon-Magnon Interaction in Low Dimensional Quantum Magnets Observed by Dynamic Heat Transport Measurements. *Phys. Rev. Lett.*, 110(14):147206, April 2013. 00000.
- [112] Gregory T. Hohensee, R. B. Wilson, Joseph P. Feser, and David G. Cahill. Magnon-phonon coupling in the spin-ladder compound $\text{Ca}_9\text{La}_5\text{Cu}_{24}\text{O}_{41}$ measured by time-domain thermoreflectance. *Physical Review B*, 89(2):024422, January 2014. 00000.
- [113] Bolin Liao, Jiawei Zhou, and Gang Chen. Generalized Two-Temperature Model for Coupled Phonon-Magnon Diffusion. *Physical Review Letters*, 113(2):025902, July 2014. 00000.
- [114] Aaron Patz, Tianqi Li, Sheng Ran, Rafael M. Fernandes, Joerg Schmalian, Sergey L. Bud’ko, Paul C. Canfield, Ilias E. Perakis, and Jigang Wang. Ultrafast observation of critical nematic fluctuations and giant magnetoelastic coupling in iron pnictides. *Nature Communications*, 5(1), feb 2014.
- [115] George D. Tsibidis. Ultrafast dynamics of non-equilibrium electrons and strain generation under femtosecond laser irradiation of nickel. *Applied Physics A*, 124(4), mar 2018.
- [116] Markus Uehlein, Sebastian T. Weber, and Baerbel Rethfeld. Implementation of the electronic non-equilibrium in the two-temperature model, 2021.
- [117] NAVINDER SINGH. Two-temperature model of nonequilibrium electron relaxation: A review. *International Journal of Modern Physics B*, 24(09):1141–1158, 2010.
- [118] Baerbel Rethfeld, Dmitriy S Ivanov, Martin E Garcia, and Sergei I Anisimov. Modelling ultrafast laser ablation. *Journal of Physics D: Applied Physics*, 50(19):193001, apr 2017.
- [119] Lutz Waldecker, Thomas Vasileiadis, Roman Bertoni, Ralph Ernstorfer, Tobias Zier, Felipe H. Valencia, Martin E. Garcia, and Eeuwe S. Zijlstra. Coherent and incoherent structural dynamics in laser-excited antimony. *Phys. Rev. B*, 95:054302, Feb 2017.
- [120] Zexi Lu, Ajit Vallabhaneni, Bingyang Cao, and Xiulin Ruan. Phonon branch-resolved electron-phonon coupling and the multitemperature model. *Phys. Rev. B*, 98:134309,

Oct 2018.

- [121] Shota Ono. Thermalization in simple metals: Role of electron-phonon and phonon-phonon scattering. *Phys. Rev. B*, 97:054310, Feb 2018.
- [122] Tobias Kampfrath, Luca Perfetti, Florian Schapper, Christian Frischkorn, and Martin Wolf. Strongly Coupled Optical Phonons in the Ultrafast Dynamics of the Electronic Energy and Current Relaxation in Graphite. *Phys. Rev. Lett.*, 95(18):187403, October 2005. 00000.
- [123] Y. Ishida, T. Togashi, K. Yamamoto, M. Tanaka, T. Taniuchi, T. Kiss, M. Nakajima, T. Suemoto, and S. Shin. Non-thermal hot electrons ultrafastly generating hot optical phonons in graphite. *Scientific Reports*, 1(1), aug 2011.
- [124] S. Dal Conte, C. Giannetti, G. Coslovich, F. Cilento, D. Bossini, T. Abebaw, F. Banfi, G. Ferrini, H. Eisaki, M. Greven, A. Damascelli, D. van der Marel, and F. Parmigiani. Disentangling the Electronic and Phononic Glue in a High-Tc Superconductor. *Science*, 335:1600, 2012.
- [125] B. Mansart, M. J. G. Cottet, G. F. Mancini, T. Jarlborg, S. B. Dugdale, S. L. Johnson, S. O. Mariager, C. J. Milne, P. Beaud, S. Grübel, J. A. Johnson, T. Kubacka, G. Ingold, K. Prsa, H. M. Rønnow, K. Conder, E. Pomjakushina, M. Chergui, and F. Carbone. Temperature-dependent electron-phonon coupling in $\text{La}_{2-x}\text{Sr}_x\text{CuO}_4$ probed by femtosecond x-ray diffraction. *Phys. Rev. B*, 88:054507, Aug 2013.
- [126] David Pines and J. Robert Schrieffer. Approach to equilibrium of electrons, plasmons, and phonons in quantum and classical plasmas. *Phys. Rev.*, 125:804, 1962.
- [127] Anatoly A. Grinberg and Serge Luryi. Nonstationary quasiperiodic energy distribution of an electron gas upon ultrafast thermal excitation. *Phys. Rev. Lett.*, 65:1251–1254, Sep 1990.
- [128] Vitaliy E. Gusev and Oliver B. Wright. Ultrafast nonequilibrium dynamics of electrons in metals. *Phys. Rev. B*, 57:2878–2888, Feb 1998.
- [129] B. Rethfeld, A. Kaiser, M. Vicane, and G. Simon. Ultrafast dynamics of nonequilibrium electrons in metals under femtosecond laser irradiation. *Phys. Rev. B*, 65:214303, May 2002.
- [130] Raseong Kim, Vasili Perebeinos, and Phaedon Avouris. Relaxation of optically excited carriers in graphene. *Phys. Rev. B*, 84:075449, Aug 2011.
- [131] B. Y. Mueller and B. Rethfeld. Relaxation dynamics in laser-excited metals under nonequilibrium conditions. *Phys. Rev. B*, 87:035139, Jan 2013.
- [132] V. V. Baranov and V. V. Kabanov. Theory of electronic relaxation in a metal excited by an ultrashort optical pump. *Phys. Rev. B*, 89:125102, Mar 2014.
- [133] Andrea Marini, Alessandro Ciattoni, and Claudio Conti. Out-of-equilibrium electron dynamics of silver driven by ultrafast electromagnetic fields – a novel hydrodynamical approach. *Faraday Discuss.*, 214:235–243, 2019.
- [134] Shota Ono and Tohru Suemoto. Ultrafast photoluminescence in metals: Theory and its application to silver. *Phys. Rev. B*, 102:024308, Jul 2020.
- [135] J. Collet and T. Amand. Model calculation of the laser-semiconductor interaction in subpicosecond regime. *Journal of Physics and Chemistry of Solids*, 47(2):153–163, 1986.
- [136] R. Binder, D. Scott, A. E. Paul, M. Lindberg, K. Henneberger, and S. W. Koch. Carrier-carrier scattering and optical dephasing in highly excited semiconductors. *Phys. Rev. B*, 45:1107–1115, Jan 1992.
- [137] Vatsal A. Jhalani, Jin-Jian Zhou, and Marco Bernardi. Ultrafast hot carrier dynamics in gan and its impact on the efficiency droop. *Nano Letters*, 17(8):5012–5019, 2017. PMID: 28737402.
- [138] Jin-Jian Zhou, Jinsoo Park, I-Te Lu, Ivan Maliyov, Xiao Tong, and Marco Bernardi. Perturbo: A software package for ab initio electron–phonon interactions, charge transport and ultrafast dynamics. *Computer Physics Communications*, 264:107970, 2021.
- [139] M. Richter, A. Carmele, S. Butscher, N. Bücking, F. Milde, P. Kratzer, M. Scheffler, and A. Knorr. Two-dimensional electron gases: Theory of ultrafast dynamics of electron-phonon interactions in graphene, surfaces, and quantum wells. *Journal of Applied*

- Physics*, 105(12):122409, 2009.
- [140] Shuntaro Tani, François Blanchard, and Koichiro Tanaka. Ultrafast carrier dynamics in graphene under a high electric field. *Phys. Rev. Lett.*, 109:166603, Oct 2012.
 - [141] D. Brida, A. Tomadin, C. Manzoni, Y. J. Kim, A. Lombardo, S. Milana, R. R. Nair, K. S. Novoselov, A. C. Ferrari, G. Cerullo, and M. Polini. Ultrafast collinear scattering and carrier multiplication in graphene. *Nat Commun*, 4(1):1987, October 2013. 00483.
 - [142] Peter Kratzer and Maedeh Zahedifar. Relaxation of electrons in quantum-confined states in Pb/Si(111) thin films from master equation with first-principles-derived rates. *New J. Phys.*, 21(12):123023, December 2019.
 - [143] Xiao Tong and Marco Bernardi. Toward precise simulations of the coupled ultrafast dynamics of electrons and atomic vibrations in materials. *Phys. Rev. Research*, 3(2):023072, April 2021.
 - [144] Fabio Caruso. Nonequilibrium lattice dynamics in monolayer mos2. *The Journal of Physical Chemistry Letters*, 12(6):1734–1740, 2021. PMID: 33569950.
 - [145] H el ene Seiler, Daniela Zahn, Marios Zacharias, Patrick-Nigel Hildebrandt, Thomas Vasileiadis, Yoav William Windsor, Yingpeng Qi, Christian Carbogno, Claudia Draxl, Ralph Ernstorfer, and Fabio Caruso. Accessing the anisotropic nonthermal phonon populations in black phosphorus. *Nano Letters*, 21(14):6171–6178, 2021. PMID: 34279103.
 - [146] B Y Mueller, T Roth, M Cinchetti, M Aeschlimann, and B Rethfeld. Driving force of ultrafast magnetization dynamics. *New Journal of Physics*, 13(12):123010, dec 2011.
 - [147] B. Y. Mueller, A. Baral, S. Vollmar, M. Cinchetti, M. Aeschlimann, H. C. Schneider, and B. Rethfeld. Feedback effect during ultrafast demagnetization dynamics in ferromagnets. *Phys. Rev. Lett.*, 111:167204, Oct 2013.
 - [148] Ting Cao, Gang Wang, Wenpeng Han, Huiqi Ye, Chuanrui Zhu, Junren Shi, Qian Niu, Pingheng Tan, Enge Wang, Baoli Liu, and Ji Feng. Valley-selective circular dichroism of monolayer molybdenum disulphide. *Nat. Commun.*, 3(1):887, January 2012.
 - [149] Kin Fai Mak, Keliang He, Jie Shan, and Tony F. Heinz. Control of valley polarization in monolayer MoS2 by optical helicity. *Nat. Nanotechnol.*, 7(8):494–498, August 2012.
 - [150] Hualing Zeng, Junfeng Dai, Wang Yao, Di Xiao, and Xiaodong Cui. Valley polarization in MoS2 monolayers by optical pumping. *Nat. Nanotechnol.*, 7(8):490–493, August 2012.
 - [151] F. Caruso, M. Schebek, Y. Pan, C. Vona, and C. Draxl. Chirality of valley excitons in monolayer transition-metal dichalcogenides. *arXiv:2112.04781*, 2022.
 - [152] Martin R. Otto, Jan-Hendrik P ohls, Laurent P. Ren e de Cotret, Mark J. Stern, Mark Sutton, and Bradley J. Siwick. Mechanisms of electron-phonon coupling unraveled in momentum and time: The case of soft phonons in TiSe₂. *Sci. Adv.*, 7(20):eabf2810, May 2021.
 - [153] Marios Zacharias, H el ene Seiler, Fabio Caruso, Daniela Zahn, Feliciano Giustino, Pantelis C. Kelires, and Ralph Ernstorfer. Multiphonon diffuse scattering in solids from first principles: Application to layered crystals and two-dimensional materials. *Phys. Rev. B*, 104:205109, Nov 2021.
 - [154] Marios Zacharias, H el ene Seiler, Fabio Caruso, Daniela Zahn, Feliciano Giustino, Pantelis C. Kelires, and Ralph Ernstorfer. Efficient first-principles methodology for the calculation of the all-phonon inelastic scattering in solids. *Phys. Rev. Lett.*, 127:207401, Nov 2021.
 - [155] J. K. Chen, J. E. Beraun. NUMERICAL STUDY OF ULTRASHORT LASER PULSE INTERACTIONS WITH METAL FILMS. *Numerical Heat Transfer, Part A: Applications*, 40(1):1–20, July 2001. 00000.
 - [156] Stefano Baroni, Stefano de Gironcoli, Andrea Dal Corso, and Paolo Giannozzi. Phonons and related crystal properties from density-functional perturbation theory. *Rev. Mod. Phys.*, 73:515–562, Jul 2001.
 - [157] S. Ponc e, E.R. Margine, C. Verdi, and F. Giustino. Epw: Electron–phonon coupling, transport and superconducting properties using maximally localized wannier functions. *Computer Physics Communications*, 209:116 – 133, 2016.
 - [158] Haining Wang, Jared H. Strait, Paul A. George, Shriram Shivaraman, Virgil B. Shields,

- Mvs Chandrashekhara, Jeonghyun Hwang, Farhan Rana, Michael G. Spencer, Carlos S. Ruiz-Vargas, and Jiwoong Park. Ultrafast relaxation dynamics of hot optical phonons in graphene. *Appl. Phys. Lett.*, 96(8):081917, February 2010.
- [159] Markus Breusing, Claus Ropers, and Thomas Elsaesser. Ultrafast Carrier Dynamics in Graphite. *Phys. Rev. Lett.*, 102(8):086809, February 2009. 00000.
- [160] John Michael Ziman. *Electrons and phonons: the theory of transport phenomena in solids*. Clarendon Press, Oxford, 1960.
- [161] S.-L. Yang, J. A. Sobota, D. Leuenberger, Y. He, M. Hashimoto, D. H. Lu, H. Eisaki, P. S. Kirchmann, and Z.-X. Shen. Inequivalence of single-particle and population lifetimes in a cuprate superconductor. *Phys. Rev. Lett.*, 114:247001, Jun 2015.
- [162] Farhan Rana. Electron-hole generation and recombination rates for coulomb scattering in graphene. *Phys. Rev. B*, 76:155431, Oct 2007.
- [163] J. M. Hamm, A. F. Page, J. Bravo-Abad, F. J. Garcia-Vidal, and O. Hess. Nonequilibrium plasmon emission drives ultrafast carrier relaxation dynamics in photoexcited graphene. *Phys. Rev. B*, 93:041408, Jan 2016.
- [164] Laura Kim, Seyoon Kim, Pankaj K. Jha, Victor W. Brar, and Harry A. Atwater. Mid-infrared radiative emission from bright hot plasmons in graphene. *Nature Materials*, 20(6):805–811, apr 2021.
- [165] J. W. McIver, B. Schulte, F.-U. Stein, T. Matsuyama, G. Jotzu, G. Meier, and A. Cavalleri. Light-induced anomalous Hall effect in graphene. *Nat. Phys.*, 16(1):38–41, January 2020.
- [166] Michael Schüler, Umberto De Giovannini, Hannes Hübener, Angel Rubio, Michael A. Sentef, Thomas P. Devereaux, and Philipp Werner. How circular dichroism in time- and angle-resolved photoemission can be used to spectroscopically detect transient topological states in graphene. *Phys. Rev. X*, 10:041013, Oct 2020.
- [167] M.A. Sentef, M. Claassen, A.F. Kemper, B. Moritz, T. Oka, J.K. Freericks, and T.P. Devereaux. Theory of Floquet band formation and local pseudospin textures in pump-probe photoemission of graphene. *Nat Commun*, 6(1):7047, November 2015. 00204.
- [168] Paul A. George, Jared Strait, Jahan Dawlaty, Shriram Shivaraman, Mvs Chandrashekhara, Farhan Rana, and Michael G. Spencer. Ultrafast Optical-Pump Terahertz-Probe Spectroscopy of the Carrier Relaxation and Recombination Dynamics in Epitaxial Graphene. *Nano Lett.*, 8(12):4248–4251, December 2008.
- [169] Dong Sun, Zong-Kwei Wu, Charles Divin, Xuebin Li, Claire Berger, Walt A. de Heer, Phillip N. First, and Theodore B. Norris. Ultrafast Relaxation of Excited Dirac Fermions in Epitaxial Graphene Using Optical Differential Transmission Spectroscopy. *Phys. Rev. Lett.*, 101(15):157402, October 2008. 00000.
- [170] Chun Hung Lui, Kin Fai Mak, Jie Shan, and Tony F. Heinz. Ultrafast Photoluminescence from Graphene. *Phys. Rev. Lett.*, 105(12):127404, September 2010. 00000.
- [171] M. Breusing, S. Kuehn, T. Winzer, E. Malić, F. Milde, N. Severin, J. P. Rabe, C. Ropers, A. Knorr, and T. Elsaesser. Ultrafast nonequilibrium carrier dynamics in a single graphene layer. *Phys. Rev. B*, 83(15):153410, April 2011. 00000.
- [172] S. Winnerl, M. Orlita, P. Plochocka, P. Kossacki, M. Potemski, T. Winzer, E. Malic, A. Knorr, M. Sprinkle, C. Berger, W. A. de Heer, H. Schneider, and M. Helm. Carrier Relaxation in Epitaxial Graphene Photoexcited Near the Dirac Point. *Phys. Rev. Lett.*, 107(23):237401, November 2011. 00000.
- [173] T. Li, L. Luo, M. Hupalo, J. Zhang, M. C. Tringides, J. Schmalian, and J. Wang. Femtosecond Population Inversion and Stimulated Emission of Dense Dirac Fermions in Graphene. *Phys. Rev. Lett.*, 108(16):167401, April 2012. 00000.
- [174] Giriraj Jnawali, Yi Rao, Hugen Yan, and Tony F. Heinz. Observation of a transient decrease in terahertz conductivity of single-layer graphene induced by ultrafast optical excitation. *Nano Letters*, 13(2):524, 2013.
- [175] A. J. Frenzel, C. H. Lui, Y. C. Shin, J. Kong, and N. Gedik. Semiconducting-to-metallic photoconductivity crossover and temperature-dependent drude weight in graphene. *Phys. Rev. Lett.*, 113:056602, Jul 2014.

- [176] S. A. Jensen, Z. Mics, I. Ivanov, H. S. Varol, D. Turchinovich, F. H. L. Koppens, M. Bonn, and K. J. Tielrooij. Competing ultrafast energy relaxation pathways in photoexcited graphene. *Nano Letters*, 14(10):5839, 2014.
- [177] Søren Ulstrup, Jens Christian Johannsen, Federico Cilento, Jill A. Miwa, Alberto Crepaldi, Michele Zacchigna, Cephise Cacho, Richard Chapman, Emma Springate, Samir Mammadov, Felix Fromm, Christian Raidel, Thomas Seyller, Fulvio Parmigiani, Marco Grioni, Phil D. C. King, and Philip Hofmann. Ultrafast dynamics of massive dirac fermions in bilayer graphene. *Phys. Rev. Lett.*, 112:257401, Jun 2014.
- [178] Isabella Gierz, Stefan Link, Ulrich Starke, and Andrea Cavalleri. Non-equilibrium dirac carrier dynamics in graphene investigated with time- and angle-resolved photoemission spectroscopy. *Faraday Discuss.*, 171:311, 2014.
- [179] I. Gierz, F. Calegari, S. Aeschlimann, M. Chávez Cervantes, C. Cacho, R. T. Chapman, E. Springate, S. Link, U. Starke, C. R. Ast, and A. Cavalleri. Tracking Primary Thermalization Events in Graphene with Photoemission at Extreme Time Scales. *Phys. Rev. Lett.*, 115(8):086803, August 2015. 00107.
- [180] Isabella Gierz, Matteo Mitrano, Hubertus Bromberger, Cephise Cacho, Richard Chapman, Emma Springate, Stefan Link, Ulrich Starke, Burkhard Sachs, Martin Eckstein, Tim O. Wehling, Mikhail I. Katsnelson, Alexander Lichtenstein, and Andrea Cavalleri. Phonon-Pump Extreme-Ultraviolet-Photoemission Probe in Graphene: Anomalous Heating of Dirac Carriers by Lattice Deformation. *Phys. Rev. Lett.*, 114(12):125503, March 2015. 00033.
- [181] Jens Christian Johannsen, Søren Ulstrup, Alberto Crepaldi, Federico Cilento, Michele Zacchigna, Jill A. Miwa, Cephise Cacho, Richard T. Chapman, Emma Springate, Felix Fromm, Christian Raidel, Thomas Seyller, Phil D. C. King, Fulvio Parmigiani, Marco Grioni, and Philip Hofmann. Tunable carrier multiplication and cooling in graphene. *Nano Letters*, 15(1):326, 2015.
- [182] S. Aeschlimann, R. Krause, M. Chávez-Cervantes, H. Bromberger, R. Jago, E. Malić, A. Al-Temimy, C. Coletti, A. Cavalleri, and I. Gierz. Ultrafast momentum imaging of pseudospin-flip excitations in graphene. *Phys. Rev. B*, 96(2):020301, July 2017. 00022.
- [183] E. Pomarico, M. Mitrano, H. Bromberger, M. A. Sentef, A. Al-Temimy, C. Coletti, A. Stöhr, S. Link, U. Starke, C. Cacho, R. Chapman, E. Springate, A. Cavalleri, and I. Gierz. Enhanced electron-phonon coupling in graphene with periodically distorted lattice. *Phys. Rev. B*, 95:024304, Jan 2017.
- [184] Takashi Someya, Hirokazu Fukidome, Hiroshi Watanabe, Takashi Yamamoto, Masaru Okada, Hakuto Suzuki, Yu Ogawa, Takushi Iimori, Nobuhisa Ishii, Teruto Kanai, Kei-ichiro Tashima, Baojie Feng, Susumu Yamamoto, Jiro Itatani, Fumio Komori, Kozo Okazaki, Shik Shin, and Iwao Matsuda. Suppression of supercollision carrier cooling in high mobility graphene on sic(000 $\bar{1}$). *Phys. Rev. B*, 95:165303, Apr 2017.
- [185] Shijing Tan, Adam Argondizzo, Cong Wang, Xuefeng Cui, and Hrvoje Petek. Ultrafast multiphoton thermionic photoemission from graphite. *Phys. Rev. X*, 7:011004, Jan 2017.
- [186] Andrea Tomadin, Sam M. Hornett, Hai I. Wang, Evgeny M. Alexeev, Andrea Candini, Camilla Coletti, Dmitry Turchinovich, Mathias Kläui, Mischa Bonn, Frank H. L. Koppens, Euan Hendry, Marco Polini, and Klaas-Jan Tielrooij. The ultrafast dynamics and conductivity of photoexcited graphene at different fermi energies. *Science Advances*, 4(5):eaar5313, 2018.
- [187] M. X. Na, A. K. Mills, F. Boschini, M. Michiardi, B. Nosarzewski, R. P. Day, E. Razzoli, A. Sheyerman, M. Schneider, G. Levy, S. Zhdanovich, T. P. Devereaux, A. F. Kemper, D. J. Jones, and A. Damascelli. Direct determination of mode-projected electron-phonon coupling in the time domain. *Science*, 366(6470):1231, 2019.
- [188] Umberto De Giovannini, Hannes Hübener, Shunsuke A. Sato, and Angel Rubio. Direct measurement of electron-phonon coupling with time-resolved arpes. *Phys. Rev. Lett.*, 125:136401, Sep 2020.
- [189] Hongyun Zhang, Changhua Bao, Michael Schüler, Shaohua Zhou, Qian Li, Laipeng Luo, Wei Yao, Zhong Wang, Thomas P Devereaux, and Shuyun Zhou. Self-energy dynam-

- ics and mode-specific phonon threshold effect in a Kekulé-ordered graphene. *National Science Review*, 09 2021. nwab175.
- [190] Umberto De Giovannini, Shunsuke A. Sato, Hannes Hübener, and Angel Rubio. First-principles modelling for time-resolved arpes under different pump–probe conditions. *Journal of Electron Spectroscopy and Related Phenomena*, 254:147152, 2022.
- [191] I. Gierz. Probing carrier dynamics in photo-excited graphene with time-resolved arpes. *Journal of Electron Spectroscopy and Related Phenomena*, 219:53–56, 2017. SI: The electronic structure of 2D and layered materials.
- [192] Isabella Gierz, Matteo Mitrano, Jesse C Petersen, Cephise Cacho, I C Edmond Turcu, Emma Springate, Alexander Stöhr, Axel Köhler, Ulrich Starke, and Andrea Cavalleri. Population inversion in monolayer and bilayer graphene. *J. Phys.: Condens. Matter*, 27(16):164204, April 2015. 00053.
- [193] Shi-Qi Hu, Hui Zhao, Chao Lian, Xin-Bao Liu, Meng-Xue Guan, and Sheng Meng. Tracking photocarrier-enhanced electron-phonon coupling in nonequilibrium. *npj Quantum Materials*, 7(1), jan 2022.
- [194] Torben Winzer, Andreas Knorr, and Ermin Malic. Carrier Multiplication in Graphene. *Nano Lett.*, 10(12):4839–4843, December 2010. 00000.
- [195] Shiwei Wu, Wei-Tao Liu, Xiaogan Liang, P. James Schuck, Feng Wang, Y. Ron Shen, and Miquel Salmeron. Hot phonon dynamics in graphene. *Nano Letters*, 12(11):5495–5499, 2012. PMID: 23106146.
- [196] Eva A. A. Pogna, Xiaoyu Jia, Alessandro Principi, Alexander Block, Luca Banszerus, Jincan Zhang, Xiaoting Liu, Thibault Sohier, Stiven Forti, Karuppasamy Soundarapandian, Bernat Terrés, Jake D. Mehew, Chiara Trovatiello, Camilla Coletti, Frank H. L. Koppens, Mischa Bonn, Hai I. Wang, Niek van Hulst, Matthieu J. Verstraete, Hailin Peng, Zhongfan Liu, Christoph Stampfer, Giulio Cerullo, and Klaas-Jan Tielrooij. Hot-carrier cooling in high-quality graphene is intrinsically limited by optical phonons. *ACS Nano*, 15(7):11285, 2021.
- [197] A. Stange, C. Sohrt, L. X. Yang, G. Rohde, K. Janssen, P. Hein, L.-P. Oloff, K. Hanff, K. Rossnagel, and M. Bauer. Hot electron cooling in graphite: Supercollision versus hot phonon decay. *Phys. Rev. B*, 92(18):184303, November 2015. 00035.
- [198] Peter Puschnig and Daniel Lüftner. Simulation of angle-resolved photoemission spectra by approximating the final state by a plane wave: From graphene to polycyclic aromatic hydrocarbon molecules. *Journal of Electron Spectroscopy and Related Phenomena*, 200:193–208, 2015. Special Anniversary Issue: Volume 200.
- [199] X. Y. Wang, D. M. Riffe, Y.-S. Lee, and M. C. Downer. Time-resolved electron-temperature measurement in a highly excited gold target using femtosecond thermionic emission. *Physical Review B*, 50(11):8016–8019, September 1994. 00412.
- [200] Federico Andreatta, Habib Rostami, Antonija Grubišić Čabo, Marco Bianchi, Charlotte E. Sanders, Deepnarayan Biswas, Cephise Cacho, Alfred J. H. Jones, Richard T. Chapman, Emma Springate, Phil D. C. King, Jill A. Miwa, Alexander Balatsky, Søren Ulstrup, and Philip Hofmann. Transient hot electron dynamics in single-layer tas_2 . *Phys. Rev. B*, 99:165421, Apr 2019.
- [201] Paulina Majchrzak, Sahar Pakdel, Deepnarayan Biswas, Alfred J. H. Jones, Klara Volckaert, Igor Marković, Federico Andreatta, Raman Sankar, Chris Jozwiak, Eli Rotenberg, Aaron Bostwick, Charlotte E. Sanders, Yu Zhang, Gabriel Karras, Richard T. Chapman, Adam Wyatt, Emma Springate, Jill A. Miwa, Philip Hofmann, Phil D. C. King, Nicola Lanatà, Young Jun Chang, and Søren Ulstrup. Switching of the electron-phonon interaction in $1t\text{-vse}_2$ assisted by hot carriers. *Phys. Rev. B*, 103:L241108, Jun 2021.
- [202] G. Grimvall. *The electron-phonon interaction in metals*. Selected topics in solid state physics. North-Holland, 1981.
- [203] P Giannozzi, O Andreussi, T Brumme, O Bunau, M Buongiorno Nardelli, M Calandra, R Car, C Cavazzoni, D Ceresoli, M Cococcioni, N Colonna, I Carnimeo, A Dal Corso, S de Gironcoli, P Delugas, R A DiStasio, A Ferretti, A Floris, G Fratesi, G Fugallo, R Gebauer, U Gerstmann, F Giustino, T Gorni, J Jia, M Kawamura, H-Y Ko, A Kokalj,

- E Küçükbenli, M Lazzeri, M Marsili, N Marzari, F Mauri, N L Nguyen, H-V Nguyen, A Otero de-la Roza, L Paulatto, S Poncé, D Rocca, R Sabatini, B Santra, M Schlipf, A P Seitsonen, A Smogunov, I Timrov, T Thonhauser, P Umari, N Vast, X Wu, and S Baroni. Advanced capabilities for materials modelling with quantum ESPRESSO. *Journal of Physics: Condensed Matter*, 29(46):465901, oct 2017.
- [204] I. Kupčić. Damping effects in doped graphene: The relaxation-time approximation. *Phys. Rev. B*, 90:205426, Nov 2014.
- [205] S. Pagliara, G. Galimberti, S. Mor, M. Montagnese, G. Ferrini, M. S. Grandi, P. Galinetto, and F. Parmigiani. Photoinduced $\pi - \pi^*$ band gap renormalization in graphite. *Journal of the American Chemical Society*, 133(16):6318–6322, 2011.
- [206] Adam T. Roberts, Rolf Binder, Nai H. Kwong, Dheeraj Golla, Daniel Cormode, Brian J. LeRoy, Henry O. Everitt, and Arvinder Sandhu. Optical characterization of electron-phonon interactions at the saddle point in graphene. *Phys. Rev. Lett.*, 112:187401, May 2014.
- [207] Fabio Caruso. Nonequilibrium lattice dynamics in monolayer mos2. *J. Phys. Chem. Lett.*, 12(6):1734–1740, 2021.
- [208] Wu Li, Jesús Carrete, Nebil A. Katcho, and Natalio Mingo. ShengBTE: a solver of the Boltzmann transport equation for phonons. *Comp. Phys. Commun.*, 185:1747–1758, 2014.
- [209] Andrea Marini, Enrico Perfetto, and Gianluca Stefanucci. Coherence and de-coherence in the time-resolved arpes of realistic materials: an ab-initio perspective, 2021.
- [210] N Schlünzen, S Hermanns, M Scharnke, and M Bonitz. Ultrafast dynamics of strongly correlated fermions—nonequilibrium green functions and selfenergy approximations. *Journal of Physics: Condensed Matter*, 32(10):103001, dec 2019.
- [211] D. M. Juraschek, M. Fechner, and N. A. Spaldin. Ultrafast structure switching through nonlinear phononics. *Phys. Rev. Lett.*, 118:054101, Jan 2017.
- [212] Giovanni Marini and Matteo Calandra. Light-tunable charge density wave orders in mote₂ and wte₂ single layers. *Phys. Rev. Lett.*, 127:257401, Dec 2021.
- [213] Meng-Xue Guan, Xin-Bao Liu, Da-Qiang Chen, Xuan-Yi Li, Ying-Peng Qi, Qing Yang, Pei-Wei You, and Sheng Meng. Optical control of multistage phase transition via phonon coupling in mote₂. *Phys. Rev. Lett.*, 128:015702, Jan 2022.
- [214] M. Nuske, L. Broers, B. Schulte, G. Jotzu, S. A. Sato, A. Cavalleri, A. Rubio, J. W. McIver, and L. Mathey. Floquet dynamics in light-driven solids. *Phys. Rev. Research*, 2:043408, Dec 2020.
- [215] Laurent P. René de Cotret, Martin R. Otto, Jan-Hendrik Pöhls, Zhongzhen Luo, Mercuri G. Kanatzidis, and Bradley J. Siwick. Direct visualization of polaron formation in the thermoelectric snse. *Proceedings of the National Academy of Sciences*, 119(3), 2022.
- [216] Niclas Schlünzen, Jan-Philip Joost, and Michael Bonitz. Achieving the scaling limit for nonequilibrium green functions simulations. *Phys. Rev. Lett.*, 124:076601, Feb 2020.
- [217] E. Perfetto, Y. Pavlyukh, and G. Stefanucci. Real-time *gw*: Toward an ab initio description of the ultrafast carrier and exciton dynamics in two-dimensional materials. *Phys. Rev. Lett.*, 128:016801, Jan 2022.